USGS
science for a changing world

Prepared in cooperation with the City of Palo Alto, California

Near-Field Receiving-Water Monitoring of Trace Metals and a Benthic Community near the Palo Alto Regional Water Quality Control Plant in South San Francisco Bay, California—2020

Open-File Report 2023–1017

U.S. Department of the Interior
U.S. Geological Survey

Cover: U.S. Geological Survey scientist collecting clams at the Baylands Nature Preserve, Palo Alto, California. Photograph by Marie-Noële Croteau, U.S. Geological Survey, December 2019.

Near-Field Receiving-Water Monitoring of Trace Metals and a Benthic Community near the Palo Alto Regional Water Quality Control Plant in South San Francisco Bay, California—2020

By Daniel J. Cain, Marie-Noële Croteau, Janet K. Thompson, Francis Parchaso, Robin Stewart, Emily L. Zierdt Smith, Kelly H. Shrader, Le H. Kieu, and Samuel N. Luoma

Prepared in cooperation with the City of Palo Alto, California

Open-File Report 2023–1017

U.S. Department of the Interior
U.S. Geological Survey

U.S. Geological Survey, Reston, Virginia: 2023

Suggested citation:
Cain, D.J., Croteau, M.-N., Thompson, J.K., Parchaso, F., Stewart, R., Zierdt Smith, E.L., Shrader, K.H., Kieu, L.H., and Luoma, S.N., 2023, Near-field receiving-water monitoring of trace metals and a benthic community near the Palo Alto Regional Water Quality Control Plant in south San Francisco Bay, California—2020: U.S. Geological Survey Open-File Report 2023–1017, 51 p., https://doi.org/10.3133/ofr20231017.

Associated data for this publication:
Cain, D.J., Croteau, M., Parchaso, F., Stewart, R., Zierdt Smith, E.L., Thompson, J.K., Kieu, L., Turner, M., and Baesman, S.M., 2022, Data for monitoring trace metal and benthic community near the Palo Alto Regional Water Quality Control Plant in South San Francisco Bay, California (ver 2.0, November 2022): U.S. Geological Survey data release, https://doi.org/10.5066/P9IBQ23S.

ISSN 2331-1258 (online)

Acknowledgments

Mark Marvin-DiPasquale, U.S. Geological Survey (USGS), provided resources for all mercury analyses. Eric Hepler (USGS), Nickolas Dulmage-Bekker (USGS), Veronika Kocen (USGS), and Matthew A.Turner (USGS), assisted with sample collections. Histological samples were prepared by Central Histology Facility, in Sacramento, California.

Contents

Figures

Tables

Conversion Factors

International System of Units to U.S. customary units

Multiply	By	To obtain
	Length	
centimeter (cm)	0.3937	inch (in.)
millimeter (mm)	0.03937	inch (in.)
meter (m)	3.281	foot (ft)
kilometer (km)	0.6214	mile (mi)
	Area	
square meter (m^2)	0.0002471	acre
	Volume	
liter (L)	33.81402	ounce, fluid (fl. oz)
liter (L)	0.2642	gallon (gal)
liter (L)	61.02	cubic inch (in^3)
	Mass	
gram (g)	0.03527	ounce, avoirdupois (oz)

Temperature in degrees Celsius (°C) may be converted to degrees Fahrenheit (°F) as follows:

$$°F = (1.8 \times °C) + 32.$$

Abbreviations

µg/g	microgram per gram
µm	micrometer
‰	parts per thousand
ANOVA	analysis of variance
CI	condition index
conf. int.	confidence interval
CV	coefficient of variation
EPA	U.S. Environmental Protection Agency
ERL	effects range low
ERM	effects range median
HCl	hydrochloric acid
HG-ICP-MS	hydride generation inductively coupled plasma mass spectrometry
ICP-OES	inductively coupled plasma optical emission spectrophotometry
MΩ•cm	megohm centimeter
MDL	method detection limit
mg/kg	milligram per kilogram
mL	milliliter
MLLW	mean lower low water
MLR	multiple linear regression
MRL	method reporting level
N	normal
NIST	National Institute of Standards and Technology
NPDES	National Pollutant Discharge Elimination System
NRCC	National Research Council Canada
PARWQCP	Palo Alto Regional Water Quality Control Plant
ppm	parts per million
RWQCB	California Regional Water Quality Control Board
SD	standard deviation
SEM	standard error of the mean
SFEI	San Francisco Estuary Institute
SRM	standard reference material
TMDL	total maximum daily loading
TOC	total organic carbon
UC	University of California
USGS	U.S. Geological Survey

Near-Field Receiving-Water Monitoring of Trace Metals and a Benthic Community near the Palo Alto Regional Water Quality Control Plant in South San Francisco Bay, California—2020

By Daniel J. Cain, Marie-Noële Croteau, Janet K. Thompson, Francis Parchaso, Robin Stewart, Emily L. Zierdt Smith, Kelly H. Shrader, Le H. Kieu, and Samuel N. Luoma

Executive Summary of Past Findings

U.S. Geological Survey (USGS) personnel have assessed trace-metal concentrations in sediments and sediment-dwelling species since 1977 at an intertidal site near the discharge of the Palo Alto Regional Water Quality Control Plant (PARWQCP). They also have profiled that area's benthic community structure since 1974. Ancillary biotic and abiotic factors that could affect metal concentrations and benthic community structure—exotic species invasions, pelagic food availability, and weather anomalies—also have been measured during this time. Collectively, this dataset describes a long-term, detailed history of metal concentrations and benthic community dynamics at this site. The executive summary, abstract, introduction, objectives, methods, and summary have been presented in previous open-file reports (for example, Dyke and others, 2012), and are summarized herein.

Initial studies during the 1970s and early 1980s found exceptionally high concentrations of silver and copper in mud-dwelling animals in this area (Luoma and Cloern, 1982; Luoma and others, 1985). Additional studies identified the PARWQCP as a point source for silver and copper and established the clam *Limecola petalum* (synonymous name *Macoma petalum*) as a biological indicator of metal exposure (Thomson and others, 1984). Elevated metal concentrations coincided with reduced reproductive activity in *L. petalum* (Hornberger and others, 2000). Related studies (Hook and Fisher 2001, 2002) supported the interpretation that elevated metal concentrations inhibited reproduction. The benthic community also showed signs of environmental stress during this time. Opportunistic organisms (capable of fast invasion and propagation in disturbed environments) dominated the community. These organisms thrived on the surface of the mud in tubes or as shelled animals, brooded their young, and fed on waterborne particles.

Concentrations of silver and copper in both sediments and tissues of *L. petalum* decreased substantially during the 1980s as the PARWQCP implemented more advanced wastewater treatment and source-control programs. Downward trends in copper concentrations in sediments and tissues of *L. petalum* correlated with reduced copper discharge from the PARWQCP (Hornberger and others, 2000; data for silver loading were not available before 1989). Coincident with the decrease in copper and silver concentrations in sediment and clams, the reproductive activity of the clam increased. The composition of the benthic community also shifted during this period. Opportunistic species became less dominant, and less opportunistic species became more persistent. Other environmental factors that vary seasonally and annually (for example, sediment composition, grain-size distribution, organic content, and ambient water salinity) were not associated with the observed temporal trends in metal concentrations, inferred metal effects on species, and benthic community changes. The only unidirectional change in an environmental factor during this period (1980–1990) was the decrease in metal loadings in the effluent discharged from the wastewater-treatment plant (Hornberger and others, 2000). The temporal coincidence between metals discharged from the plant, metal concentrations in sediment and tissues of *L. petalum* at the site, and the observed biological responses suggested that the recession in metal exposure was principally responsible for the observed biological recovery.

After the significant reductions in the 1980s, concentrations of silver and copper in sediments and *L. petalum* continued to decrease, although much more gradually. However, silver concentrations in sediments remain greater than what is considered the natural regional background (0.09±0.02 milligram per kilogram [mg/kg]) (Hornberger and others, 1999). The concentrations of silver and copper in *L. petalum* have fluctuated as much as fourfold since 1994. Some of the interannual variation in silver concentrations of *L. petalum* appears related to annual growth and reproductive cycles independently of exposure. Copper concentrations did not appear responsive to either modest changes in sedimentary copper or growth and reproductive cycles.

Biological responses coincident with the decrease and stabilization of silver and copper exposures were evident. Reproductive activity of *L. petalum* increased (Hornberger

and others, 2000). Structural and functional attributes of the benthic community shifted from a taxa assemblage dominated by a few surface-dwelling, brooding species to species with various life-history characteristics. In particular, species that lay their eggs in the mud and feed by burrowing through and consuming the mud, which were rare in the community in the 1970s and 1980s, have increased in abundance. Today (2020), the community at this site is very similar to the benthic community observed by Thompson and Parchaso (2012) throughout south San Francisco Bay.

When the trace metal study started in the late 1970s, the site was already heavily contaminated. Although we assume that the biological conditions reflected the consequences of elevated metal exposures, preexisting data to evaluate the effects of elevated metal exposure is scarce, particularly over decadal time scales. However, the long-term record contained in this study provides a unique opportunity to document biological response when the stress of metal exposure is relaxed. The data—together with complementary studies—make a compelling case that the mitigation of silver and copper in wastewater effluent during the 1980s allowed for biological recovery and the establishment of a more diverse and stable infaunal community.

Abstract

Trace-metal concentrations in sediment and in the clam *Limecola petalum* (World Register of Marine Species, 2020; formerly reported as *Macoma balthica* and *M. petalum*), clam reproductive activity, and benthic macroinvertebrate community structure were investigated in a mudflat 1 kilometer (km) south of the discharge of the Palo Alto Regional Water Quality Control Plant (PARWQCP) in south San Francisco Bay, California. This report includes the data collected by the U.S. Geological Survey (USGS) for January 2020–December 2020 (Cain and others, 2022). These data append to long-term datasets extending back to 1974. A major focus of the report is an integrated description of the 2020 data within the context of the longer, multidecadal dataset. This dataset supports the City of Palo Alto's Near-Field Receiving-Water Monitoring Program, initiated in 1994.

Silver and copper contamination substantially decreased at the site in the 1980s following the implementation by PARWQCP of advanced wastewater-treatment and source-control measures. Since the 1990s, concentrations of these elements in surface sediments have continued to decrease, although more slowly. For example, from 1994 to 2020, the minimum annual mean silver concentration—0.20 milligram per kilogram (mg/kg)—was observed in multiple years. In 2020, silver concentrations ranged from 0.18 to 0.28 mg/kg. These concentrations are 2 to 3 times higher than the regional background concentration. Presently (2020), sediment-copper concentrations appear to be near the regional background level. Over the same period (1994–2020), sedimentary iron and zinc exhibited modest decreases. Sedimentary aluminum, chromium, mercury, nickel, and selenium have not exhibited any trend. Since 1994, silver and copper concentrations in *L. petalum* have varied seasonally, apparently in response to a combination of site-specific metal exposures and cyclic growth and reproduction, as reported previously. Seasonal patterns for other elements, including chromium, mercury, nickel, selenium, and zinc, generally were similar in timing and magnitude as those for silver and copper. Downward trends in the silver and zinc concentrations in *L. petalum* during 1994–2020 were evident and appeared to be related to the general physiological condition of the clam, indicated by a condition index.

Biological effects of elevated silver and copper contamination at the Palo Alto site have been interpreted from data collected during and after the recession of these contaminants. Concentrations of both elements in the soft tissues of *L. petalum* decreased with sedimentary copper and silver. This pattern was associated with changes in the reproductive activity of *L. petalum*, as well as the structure of the benthic invertebrate community. Reproductive activity of *L. petalum* increased as metal concentrations in *L. petalum* decreased (Hornberger and others, 2000), and presently is stable with almost all animals initiating reproduction in the fall and spawning the following spring. Analyses of the benthic community structure indicate that the infaunal invertebrate community has shifted from one dominated by several opportunistic species when silver and copper exposures were highest to one in which the species abundance is more evenly distributed, a pattern that indicates a more stable community that is subjected to fewer stressors. Importantly, this long-term change is unrelated to other metals and other measured environmental factors, including salinity and sediment composition. In addition, two of the opportunistic species (*Ampelisca abdita* and *Streblospio benedicti*) that brood their young and live on the surface of the sediment in tubes have shown a continual decrease in dominance coincident with the decrease in metals. Both species had short-lived rebounds in abundance in 2008, 2009, and 2010 and showed signs of increasing abundance in 2020. *Heteromastus filiformis* (a subsurface polychaete worm that lives in the sediment, consumes sediment and organic particles residing in the sediment, and reproduces by laying its eggs on or in the sediment) showed a concurrent increase in dominance and, in the last several years before 2008, showed a stable population. *H. filiformis* abundance increased slightly from 2011 to 2012 and returned to pre-2011 numbers in 2020.

The reproductive mode of most species that were present in 2020 was indicative of species that were capable of movement either as pelagic larvae or as mobile adults. Although oviparous species were lower in number in this group, the authors hypothesize that these species will return slowly as more species move back into the area. The use of functional ecology was highlighted in the 2020 benthic community data, which showed that the animals that have now returned to the mudflat are those that can respond successfully to a physical, nontoxic disturbance. Today, community data show a mix of species that consume the sediment, or filter

feed, those that have pelagic larvae that must survive landing on the sediment, and those that brood their young. The long-term recovery observed after the 1970s can be ascribed to the decrease in sediment pollutants.

Introduction

Determining spatial distributions and temporal trends in trace metals in sediments and benthic organisms is common practice for monitoring environmental contamination. These data can be the basis for assessing metal exposure, the potential for adverse biological effects, and the response to regulatory or management actions (Suter, 2001). Another common method of environmental monitoring is to examine the community structure of sediment-dwelling benthic organisms (Simon, 2002). Spatial and temporal changes in community structure reflect the integrated response of resident species to environmental conditions, although the underlying cause(s) for the response may be difficult to identify and quantify. Together, measurements of metal exposure and biological response can provide a more complete view of anthropogenic disturbances and the associated effects on ecosystem health.

Sediment particles can strongly bind metals, effectively repartitioning them from solution to a solid phase. As a result, sediments may accumulate and retain metals released to an aquatic environment. Sediment cores provide a historical record of metal inputs that can reveal anthropogenic influences (Förstner and Wittmann, 1981). Specifically, studies of sediment cores in San Francisco Bay chronicled metal inputs and suggested that legacy contamination can remain a chronic source of metals to the system owing to sediment mixing and redistribution (Hornberger and others, 1999; van Geen and Luoma, 1999). Metals in sediments also indicate exposure levels to benthic animals through contact with, and ingestion of, bottom sediments and suspended particulate materials. However, physical and geochemical conditions of the sediment affect the biological availability of the bound metals. Assimilation of bioavailable sediment-bound metal by digestive processes and the contribution of this source of metals relative to metals in the aqueous phase are difficult to predict from sediment concentrations alone. Thus, in order to better estimate bioavailable metal exposures, the tissues of the organisms themselves may be analyzed for trace metals (Phillips and Rainbow, 1993). Different species concentrate metals to different degrees. However, if one species is analyzed consistently, the results can be used to track temporal changes in trace-element exposures at a specified location.

Contaminants can adversely affect benthic organisms at several organizational levels. For example, responses to a pollutant at the cellular or physiological level of an individual can cause changes at the population level, such as reductions in growth, survival, and reproductive success (Newman, 1998). Community-level responses to population-level impairment can include overall shifts in diversity and species abundance, favoring metal-tolerant species, which can result in changes in predator-prey interactions and competition for available resources. Changes in the benthic community can ultimately result in changes at the ecosystem level because of that community's importance as primary consumers in the cycling of carbon in aquatic environments (Alpine and Cloern [1992] provided a local example).

In all aquatic environments, benthic organisms may be exposed to contaminants at all life stages through a variety of routes—sediment, water, and food (Wang and Fisher [1999] provided a summary of the potential transport of trace elements through food). Toxicant exposure is related to contaminant concentration and time (frequency and duration of exposure). Even at fairly low contaminant levels, long-term exposure can affect benthic organisms (Long and others, 1995). The added complexity of synergistic or antagonistic effects between different contaminants, and between contaminants and natural stressors, makes causal relationships difficult to identify and quantify, even on a site-specific basis. However, long-term monitoring can provide a time-integrated portrayal of ecosystem response to contaminant loading that links changes in exposure at multiple time scales (in this case, seasonal to decadal) to changes at individual, population, and community levels. Data from such studies support surveillance and compliance of water-quality objectives.

Permits issued by the California Regional Water Quality Control Board (RWQCB) under the National Pollutant Discharge Elimination System (NPDES) to the Palo Alto Regional Water Quality Control Plant (PARWQCP) (fig. 1) require a prescribed self-monitoring program. In addition, the City of Palo Alto augments its own monitoring program with data collected by the U.S. Geological Survey (USGS). The USGS monitoring protocols have been designed to be compatible with or complementary to the RWQCB's Regional Monitoring Program. In this report, the USGS monitoring study is described and data collected during 2020 are presented within the context of more than 44 years of previous data collections and investigations by the USGS at this intertidal location.

The data collected during this study include trace-metal concentrations in sediments and clams, clam reproductive activity, and benthic community structure (based on taxonomic analyses). These data and those reported earlier (for example, Luoma and others, 1991, 1995a, 1996; Hornberger and others, 2000; Thompson and others, 2002; Shouse and others, 2003, 2004; Moon and others, 2005; Cain and others, 2006, 2021; Dyke and others, 2012, 2014) were used to meet the following objectives:

- Provide data to assess seasonal and annual trends in trace-element concentrations in sediments and clams, reproductive activity of clams, and benthic community structure at a site designated in the RWQCB's self-monitoring program guidelines for PARWQCP.
- Present the data within the context of historical changes in south San Francisco Bay and within the context of other locations in the bay published in the international literature.

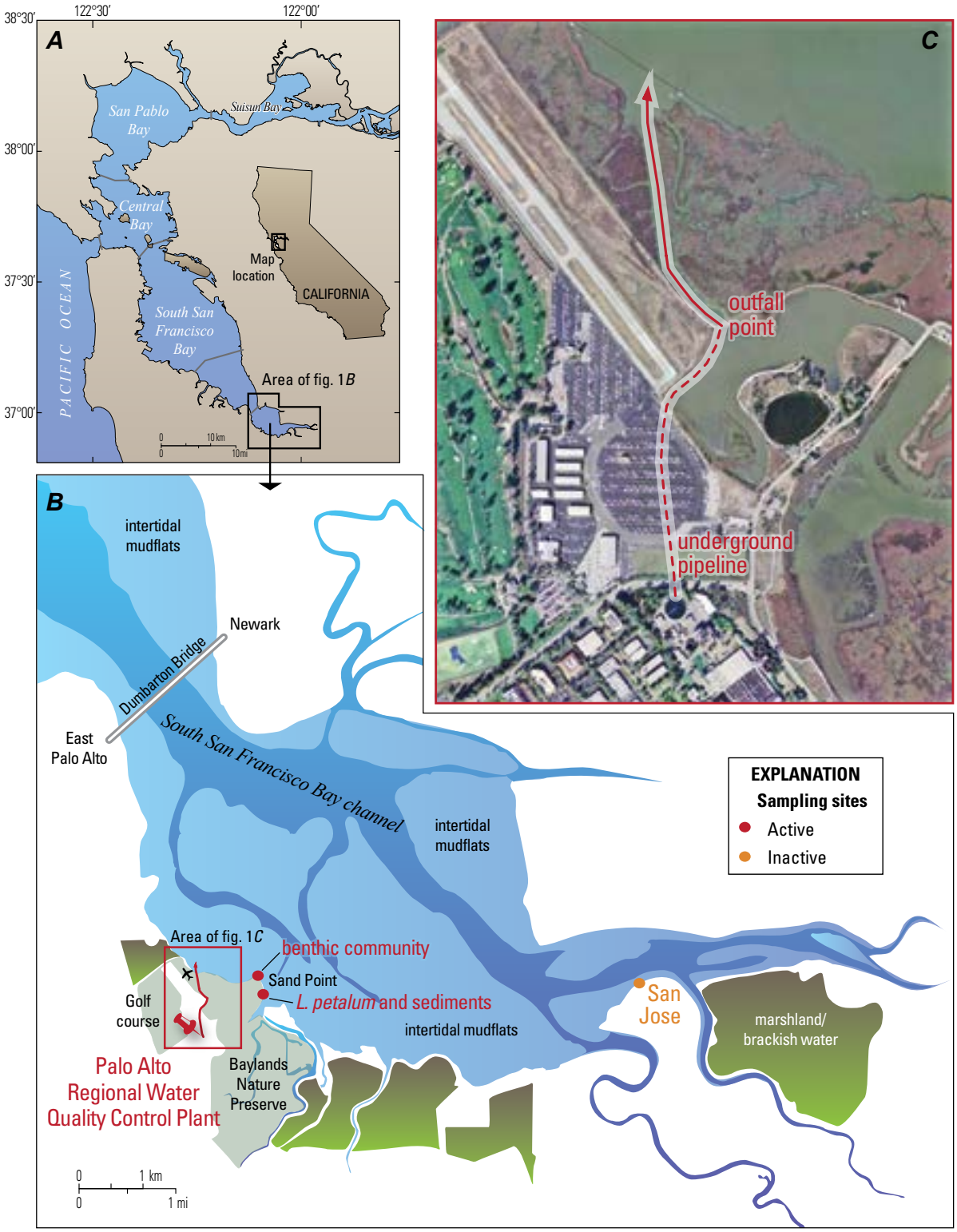

Figure 1. Location of Palo Alto site in south San Francisco Bay, California (from Dyke and others, 2010). *A*, Map showing location of sampling areas (and fig. 1*B*) within greater San Francisco Bay region. *B*, Map showing Palo Alto sampling sites, which consist of benthic community at Sand Point and clam *Limecola petalum* and sediments localities a few hundred meters south of it; inactive sampling site shown for reference. Palo Alto Regional Water Quality Control Plant (located at red thumbtack) and extent of surrounding area are shown in figure 1*C*. *C*, Satellite image showing Palo Alto Regional Water Quality Control Plant (red thumbtack in 1*B*) (source of satellite image: Google Earth). Effluent from plant is discharged by way of underground pipe (dashed line) until it reaches outfall point at mouth of small channel, which flows (red arrow) through intertidal mudflat to bay, about 1 kilometer (km) west-northwest of sampling sites.

- Coordinate an inshore receiving-water monitoring program for PARWQCP and provide data compatible with relevant aspects of the regional monitoring program. The near-field data will augment the regional monitoring program as suggested by the RWQCB.

- Provide data that could support other south San Francisco Bay management issues or programs, such as total maximum daily loading (TMDL) targets.

Despite the complexities inherent in monitoring natural systems, the adopted approach has been effective in relating changes in near-field contamination to changes in reproductive activity of a clam (Hornberger and others, 2000) and in benthic community structure (Kennish, 1998). This study, with its basis in historical data, provides a rare multidecadal context within which future environmental changes can be assessed.

Metal concentrations were monitored in sediments and a resident clam species, *Limecola petalum*. Analysis of trace-metal concentrations in the sediments over time provides a record of metal contamination at the site. The concentration and bioavailability of sediment-bound metals are affected by physical and geochemical factors (Thomson-Becker and Luoma, 1985; Luoma and others, 1995b). Thus, ancillary data, including grain-size distribution, organic carbon, aluminum and iron content of the sediment, regional rainfall, and surface salinity were collected to interpret seasonal, annual, and interannual variation in metal concentrations. The tissue of *L. petalum* provides an estimate of internalized metal (dose), which is an indication of exposure to bioavailable metals. Although the measured metal concentrations are specific to *L. petalum*, they serve as a relative indicator of metal exposure to the broader benthic invertebrate community.

Biological response of the benthic community to metal exposure was examined at three levels of organization: individual, population, and community. At the individual level, concentrations of metals in the tissues of *L. petalum* were compared with physiological indicators. Two common animal responses to environmental stress are reductions in both growth and reproductive activity. Growth and reproduction in *L. petalum* occur on fairly regular seasonal cycles. Seasonally, a clam of a given shell length will increase somatic tissue weight as it grows during the late winter and spring (Cain and Luoma, 1990). Reproductive tissue increases during the early stages of reproduction and decreases during and after spawning. These cycles can be followed with the condition index (CI), which is represented as the total soft-tissue weight of a clam standardized to shell length and is indicative of the physiological condition of the animal (Cain and Luoma, 1990). Interannual differences in growth and reproduction, expressed in the CI, are affected by the availability and quality of food, as well as other stressors, such as pollutant exposure and salinity extremes. Hornberger and others (2000) showed that reproductive activity of *L. petalum* increased with decreasing metal concentrations in animals from this location. Therefore, CI and reproductive activity of *L. petalum* appear to be useful indicators of physiological stress by pollutants at this location, and they continue to be monitored in this study.

At the population level, trends of the dominant benthic species were examined to see if certain species have been more affected than others by environmental change. Studies have shown that most taxonomic groups have species that are sensitive to elevated silver (Luoma and others, 1995b) and that some crustacean and polychaete species are particularly sensitive to elevated sedimentary copper (Rygg, 1985; Morrisey and others, 1996). In addition, the benthic community was examined for changes in structure—that is, shifts in the species composition of the macroinvertebrate community that typically result in a change in the function of that community. We hypothesized that a change in the exposure to contaminants, particularly metals, could alter community structure and function. First, prior studies have shown that south San Francisco Bay benthic communities were dominated by opportunistic species in the 1980s (Nichols and Thompson, 1985a). These opportunistic species might become less dominant as environmental stressors decrease. Second, environmental pollutants may differentially affect benthic species that use different feeding and reproductive modes. An intertidal mudflat community, such as this study site, should include a combination of species that feed on particles in the water column, on settled and buried food particles in the mud, and on other organisms. The absence of any one of these feeding groups may indicate a limitation on species resulting from specific environmental stressors. For example, pollutants attached to sediment particles are more likely to affect species that consume the sediment as part of their feeding mode or those species that lay their eggs in the sediment.

Previous analysis of this community has shown no correlation between changes in the community and measured environmental parameters (salinity, air and water temperature, delta outflow, precipitation, chlorophyll a, sediment total organic carbon, and biological oxygen demand; Shouse, 2002). Therefore, the community data are compared only to trace-metal data in this report.

The Palo Alto site, which is located on a mudflat on the western shore of San Francisco Bay, includes the benthic community sampling site and the *L. petalum* and sediment sampling site, both adjacent to Sand Point in Palo Alto Baylands Nature Preserve on a mudflat on the western shore of San Francisco Bay (fig. 1). The site is 1 kilometer (km) southeast of the intertidal discharge point of the PARWQCP. The sampling sites are approximately 12 meters (m) from the edge of the marsh and 110 centimeters (cm) above mean lower low water (MLLW).

The sediment and biological samples from this location reflect a response of the receiving waters to the effluent just beyond the location of discharge. Earlier studies (Thomson and others, 1984) showed that dyes, natural organic materials in San Francisquito Creek, and waters in the PARWQCP discharge move predominantly southward toward Sand Point, thereby affecting the mudflats near Sand Point. Thomson and others (1984) showed that San Francisquito Creek and

the Palo Alto Yacht Harbor were minor sources of most trace elements compared to the PARWQCP. On the basis of spatial and temporal trends of copper, silver, and zinc in clams and sediments, the PARWQCP appeared to be the primary source of elevated metal concentrations at the Palo Alto site in the spring of 1980 (Thomson and others, 1984; Cain and Luoma, 1990). Metal concentrations in sediments and clams (*L. petalum*), especially silver and copper, have decreased substantially since the original studies as more efficient treatment processes and source controls were used (Hornberger and others, 2000). Frequent sampling each year was necessary to characterize those trends because of significant seasonal variability (Luoma and others, 1985; Cain and Luoma, 1990). This report characterizes data for the year 2020, thereby extending the long-term record at this site.

Methods

Sampling Frequency and Duration

In dynamic ecosystems such as San Francisco Bay, the environmental effects of anthropogenic stressors are difficult to distinguish from natural seasonal or life-cycle changes. Sustained sampling at frequent intervals can characterize seasonal patterns, capture episodic events, and identify longer term trends, thereby increasing the probability that anthropogenic effects can be identified. Analyses of early community data (1974–1983; Nichols and Thompson, 1985a, 1985b) showed that benthic samples need to be collected at monthly to bimonthly intervals to distinguish between natural and anthropogenic effects. Therefore, data reported herein are based on samples collected on a semimonthly basis from the exposed mudflat at low tide between January and December (Cain and others, 2022). Samples include surface sediment, the deposit-feeding clam *L. petalum*, surface water, and sediment cores for community analysis. Data on sediments, *L. petalum*, and surface water have been collected continuously since 1977, whereas community data were collected from 1974 to 1990 and from 1998 to the present (2020).

Measurements of Metal Exposure

Metal concentrations in surficial sediments and in the soft tissues of *L. petalum* were interpreted as indicative of metal exposure to the broader benthic community. The collection and preparation of sediment and *L. petalum* samples have been previously described in detail (for example, Dyke and others, 2014; Cain and others, 2021). The next sections are an overview of those procedures.

Surface Sediment

Sediment samples were collected from the visibly oxidized (brownish) surface layer (top 1–2 cm) of mud and later that day sieved through a 100-micrometer (µm) mesh polyethylene screen with distilled water to remove large grains that might bias interpretation of concentrations. The mesh size was selected to match the largest grains typically found in the digestive tract of *L. petalum*. All chemical data reported herein were determined from the fraction that passed through the sieve (<100 µm), termed the "silt/clay fraction."

The percentage of silt/clay fraction of sediment samples was determined to provide some comparability with bulk-sediment determinations such as that used in the Regional Monitoring Program (San Francisco Estuary Institute, 1997). The sediment that did not pass through the sieve (≥100 µm)—termed the sand fraction—was collected, as was the silt/clay fraction (<100 µm) (see previous paragraph). Each fraction was dried to constant weight, and their percentage of contributions to the bulk sample was determined gravimetrically.

The silt/clay fraction was subsampled to provide replicates weighing 0.2 to 0.3 grams (g). These were redried (70 °C), reweighed, and then digested by hot acid reflux (10 milliliters [mL] of 16 normal [N] nitric acid). This method provides a "near-total" extraction of metals from the sediment and is comparable to the recommended procedures of the U.S. Environmental Protection Agency (EPA) (U.S. Environmental Protection Agency, 1994, 1996) and to the procedures used in the regional monitoring program (for example, San Francisco Estuary Institute, 2016). Another set of replicate subsamples from the silt/clay fraction were directly extracted with 12 mL of 0.6 N hydrochloric acid (HCl) for 2 hours at room temperature. This partial extraction method extracts metals bound to sediment surfaces and is operationally designed to obtain a crude chemical estimate of bioavailable metal.

The organic carbon content of surficial sediment was determined by flow isotope ratio mass spectrophotometry at the University of California (UC) at Davis Stable Isotope Facility. Weighed samples of dry, pulverized sediment were fumigated in a hydrochloric acid atmosphere overnight at the USGS metal bioavailability laboratory in Menlo Park, California, and then shipped to the UC Davis Stable Isotope Facility for analysis (see https://stableisotopefacility.ucdavis.edu for more information).

Clam Tissue

Specimens of *L. petalum* were collected by hand and placed into containers with site water. Typically, 60 to 120 individual clams were collected, representing a range of sizes (shell length). In the laboratory, clams were removed from containers and gently rinsed with deionized water to remove sediment. Clams were immersed in seawater diluted with deionized water as necessary to reach the equivalent of ambient salinity and moved to a constant-temperature room (12±1 °C) for 48 hours to allow for the egestion of sediment and undigested material from their digestive tracts.

Sample Preparation for Metal Analysis, Excluding Mercury and Selenium

The shell length of each clam was measured with electronic calipers and recorded digitally. Clams were separated into 1- or 2-millimeter (mm) size classes (for example,

10.00–10.99 mm or 11.00–11.99 mm). The soft tissues from all individuals within a given size class were dissected from the shell and collected in preweighed acid-washed 20-mL screw-top borosilicate glass vials to form a single composite sample for elemental analysis. The vials were transferred to a convection oven (60±1 °C). After the tissues were dried to constant weight, they were digested by reflux in subboiling 16 N nitric acid. The tissue digests were then dried, and the metals were resolubilized in 0.6 N HCl for trace-metal analysis.

Analytical, Excluding Mercury and Selenium

Sediment and tissue concentrations of aluminum, chromium, copper, iron, nickel, silver, and zinc were determined using inductively coupled plasma optical emission spectrophotometry (ICP-OES). Samples and standard reference materials were filtered (0.45 µm) prior to analysis.

Sample Preparation and Analysis for Mercury and Selenium

Approximately 40 clams were selected from each collection. The only criterion for selection was that the range of sizes (shell length) within this group was representative of the larger collection. Otherwise, the selection of individuals was random. Selected individuals were grouped according to size to form three composites, each containing a minimum of approximately 1.25 g wet weight. To meet this requirement, especially for small clams, the 1-mm size classes were usually combined to form broader size classes (within 3–4 mm of each other, as appropriate). Once the composites were formed, the soft tissues of the clams were dissected from the shell and placed into 10-mL screw-top polycarbonate vials. A small volume (2–3 mL) of double-deionized water (approximately 18 megohm centimeter [MΩ•cm] resistivity) was then added to the sample and subsequently homogenized with a high-speed tissue homogenizer. Once homogenized, the samples were refrozen (−80 °C) and then freeze-dried.

Sediment samples for mercury and selenium analyses were prepared with the same methods used for other trace elements (described in the "Surface Sediment" section and in previous reports; for example, Dyke and others, 2014; Cain and others, 2021).

Tissue and sediment samples were subsampled and analyzed for total mercury by acid-digestion, BrCl oxidation, purge and trap, and cold vapor atomic fluorescence spectrometry according to the EPA Method 1631, Revision E (U.S. Environmental Protection Agency, 2002), and for selenium by acid digestion, hydrogen peroxide oxidation, hydride generation inductively coupled plasma mass spectrometry (HG-ICP-MS) according to a method modified from Elrick and Horowitz (1985), which was published by Kleckner and others (2017).

Quality Assurance

All glass and plastic materials used in the collection, preparation, and storage of samples were first cleaned thoroughly to remove metal contamination. Cleaning consisted of sequential immersion in a detergent bath for at least 24 hours, a rinse in deionized water, then immersion in a 10-percent HCl wash for at least 24 hours, followed by a thorough rinse in double-deionized water. Materials were dried in a dust-free, positive-pressure environment, sealed, and stored in a dust-free cabinet.

Samples prepared for ICP-OES analysis (that is, all elements except selenium and mercury) were accompanied by procedural blanks, spiked procedural blanks and samples, and standard reference materials (SRMs) issued by the National Institute of Standards and Technology (NIST) and the National Research Council Canada (NRCC) (Cain and others, 2022). Analysis was preceded by instrument calibration, followed by quality-control checks with prepared quality-control standards before, during (approximately every 10 samples), and after each analytical run. Metal recoveries of sediment digests were evaluated with NIST 2709a San Joaquin soil and NIST 2711a Montana II soil (appendix 1). Metal recoveries for soft-tissue digests were evaluated with NIST 1566b oyster tissue and NRCC TORT-3 lobster hepatopancreas (appendix 2). Results were consistent within methods. Recoveries of silver, copper, nickel, and zinc from NIST 2709a and 2711a by the near-total extraction method generally were consistent with those reported by NIST for EPA methods 200.7 and 3050B, whereas the near-total extraction method recovered a greater percentage of total aluminum, chromium, and iron. Recoveries of elements in biological SRMs were consistently greater than 80 percent.

Analytical precision of mercury and selenium methods were determined in sample splits (appendix 3). Coefficients of variation were less than or equal to 1.56 percent.

A variety of SRMs were prepared according to the method used for the determination of selenium and mercury. Mean selenium recoveries for respective biological and sediment SRMs were 100 to 104 percent and 108 percent, respectively, whereas mean mercury recoveries were 90 to 118 percent and 89 percent, respectively (appendix 4).

Method detection limits (MDL) and method reporting levels (MRL) for ICP-OES methods were determined using the procedures outlined by Glaser and others (1981), Childress and others (1999), and U.S. Environmental Protection Agency (2004) (appendix 5).

Salinity

A small volume (approximately 25 mL) of water pooled on the surface of the mudflat was collected in a polypropylene bottle and returned to the laboratory, where salinity was measured with a handheld refractometer. Additionally, salinity

is determined in a small volume (approximately 1–2 mL) of bay water collected from the body cavity of *L. petalum*. Salinity of the surface-water sample and the body-water sample consistently agreed within 1 part per thousand (‰) for most months.

Other Data Sources

Precipitation data for San Francisco Bay are reported from a station at San Francisco International Airport (San Francisco WB AP, station identification SFF) and were obtained from the California Data Exchange Center (http://cdec.water.ca.gov/).

Biological Response

Condition Index

The CI is a measure of the clam's physiological state derived from the relation between soft-tissue weight and shell length and reported as the soft-tissue dry weight (in grams) for a clam of a particular shell length (in millimeters [mm]). Specifically, for each collection, the relation between the average shell length and tissue dry weight of the composites was fit with a linear regression, and from that regression, the tissue dry weight was predicted for a normalized shell length of 25 mm (Cain and Luoma, 1990).

Reproductive Activity

A minimum of 10 clams of varying sizes (≥10 mm shell length) were processed for reproductive activity concurrent with samples for metal analyses. Clams were immediately preserved in 10-percent formalin at the time of collection. The visceral mass of each clam was removed in the laboratory, stored in 70-percent ethyl alcohol. Samples were shipped to a commercial laboratory (Central Histology Facility, Sacramento, Calif.) where they were prepared using standard histological techniques. Tissues were dehydrated in a graded series of alcohol, cleared in toluene (twice for 1 hour each), and infiltrated in a saturated solution of toluene and Paraplast for 1 hour, and two changes of melted Tissuemat for 1 hour each. Samples were embedded in Paraplast in a vacuum chamber and then thin-sectioned (10 µm) using a microtome (Weesner, 1960). Sections were stained with Harris' hematoxylin and eosin and examined with a light microscope. Each individual was characterized by size (length in mm), sex, developmental stage, and condition of gonads, thus allowing each specimen to be placed in one of five qualitative classes of gonadal development (Parchaso, 1993).

Community Analysis

Samples for benthic community analysis were collected with a hand-held core, 8.5 cm in diameter and 20 cm deep. Three replicate samples were taken within a 1 square meter (m^2) area, defined as "the station," during each sampling date. Core placement was based on a rotating pattern in which the cores were placed on different sides of the station each month, allowing the sampling area enough time to recover, to provide an accurate representation of the benthic community. The sampling locations were (in sampling order) southeast of the station, northwest of the station, southwest of the station, and northeast of the station (Cain and others, 2021).

Benthic community samples were washed and retained on a 500-µm screen, fixed in 10-percent formalin, and then later preserved in 70-percent ethanol. Samples were stained with rose bengal solution. All animals in all samples were sorted to species level where possible, and individuals for each species were enumerated. However, some groups, such as the oligochaetes, are still not well defined in the bay; hence, they were not enumerated to the species level. Taxonomic work was performed by Sarah Pearson (West Sacramento, Calif.) under contract to the U.S. Geological Survey. Pearson is a private contractor familiar with the taxonomy of San Francisco Bay invertebrates. She compared and verified her identifications with previously identified samples.

Statistical Analysis

Metals data are reported as monthly means with associated standard deviations (SD) and annual (grand) means of monthly means with associated standard error of the mean (SEM). In instances where more than one sample was collected within a single month (for example, 1977–1980), the mean of those samples was calculated to harmonize the data to the study design implemented in 1994, which collects one sample within a given month. Throughout the report, metals data are illustrated to represent interannual variation for the period of record (for silver and copper, 1977–2020, and for other metals, 1994–2020) and intra-annual variation over the past 5 years. The general patterns of seasonal variation were based on monthly means of all samples collected from 1994 to 2020. Data were standardized for Pearson product-moment correlation. The annual mean-metal concentrations of *L. petalum* were examined for trends from 1994 to 2020. Data were checked for normality using the Shapiro-Wilk W statistic and transformed, as needed, for Pearson product-moment correlation. If transformations failed to distribute the data normally, data were analyzed with nonparametric correlation (Spearman rank). Variables affecting interannual trends in metal concentrations of *L. petalum* were analyzed using multiple linear regression (MLR). Statistical analyses were performed with Statistica v. 13.2 (Dell Inc., 2016). Differences with a Type I error rate $\alpha \leq 0.05$ were considered significant. Estimated taxa density and abundance are scaled to 1 m^2 and reported as the mean ±SD (n=3) of the replicate cores.

Results

Salinity

Surface-water salinity in the bay is related to, and roughly the inverse of, the seasonal weather pattern in northern California, which is characterized by a winter rainy season that

has been defined as months with rainfall amounts greater than 0.25 inches (in.) (November through April) and a summer dry season (May through October). Total precipitation measured at station SFF in 2020 was 5.85 in. (fig. 2). Salinity ranged from 24 to 30 parts per thousand during 2020 (fig. 3).

Sediments

Surficial sediment collected in this study is dominated by silt- and clay-sized particles (<100 µm), averaging 80 percent of the sampled sediment on a dry-weight basis (table 1). These fine sediments provide large surface areas for metal sorption. Concentrations of sorbed metals vary as a function of the ratio of surface area to volume of a particle and, thus, tend to track the percentage of fine particles. Within years, metal concentrations and total organic carbon (TOC) typically are highest in winter-spring and lowest in summer-fall (fig. 4). Thomson-Becker and Luoma (1985) suggested that intra-annual variation in sediment metal concentration at the Palo Alto site is related to changes in the size distribution of sediment particles caused by allochthonous inputs and deposition of fine-grained particles in the winter and their subsequent wind-driven resuspension in the summer and fall. This explanation is supported by the seasonal periodicity displayed by the percentage of fine particles, aluminum and iron concentrations (fig. 5), and other metals considered in this study (not illustrated). With the exception of mercury, the seasonal patterns in the concentration of individual metals and the percentage of fine-grained material correlate (r=0.81–0.92, p<0.05).

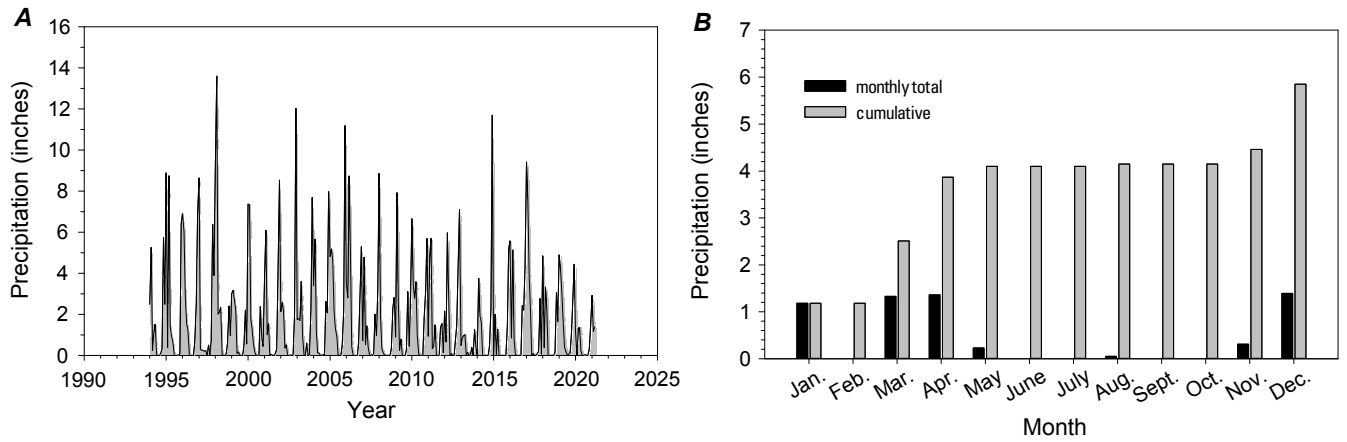

Figure 2. Graphs showing precipitation, in inches, recorded at station San Francisco WB AP, San Mateo County, California *A*, Annual precipitation, 1994–2020. *B*, Monthly and cumulative precipitation, 2020. The station (identification, SFF; San Francisco WB AP [SFF] [https://cdec.water.ca.gov/dynamicapp/selectQuery?Stations=SFF&SensorNums=2&dur_code=M&Start=2021-03-13&End=2023-03-13]) is operated by National Weather Service.

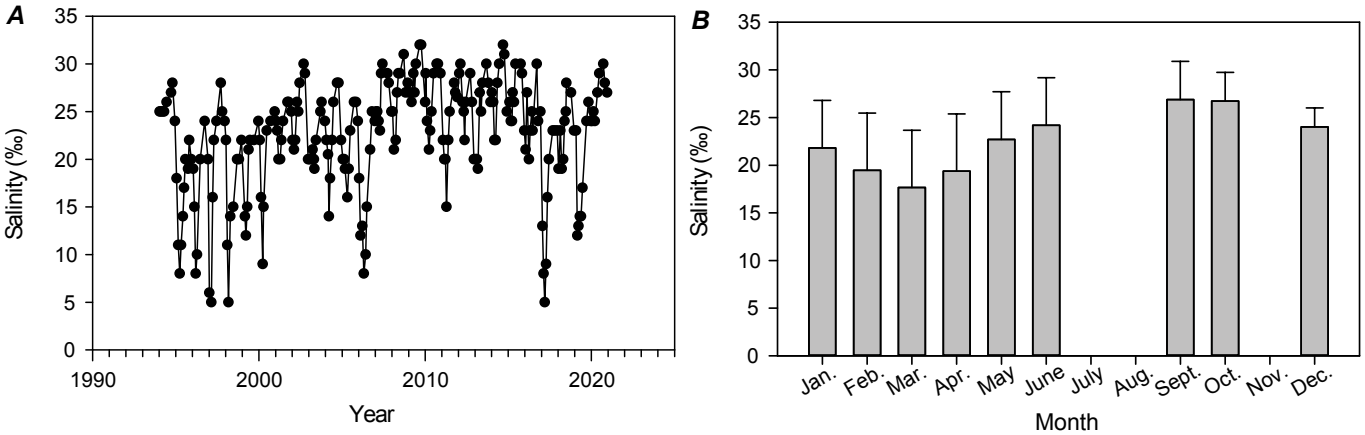

Figure 3. Surface-water salinity, in parts per thousand (‰), at Palo Alto site, California, 1994–2020. *A*, Monthly data. *B*, Boxplots showing general seasonal variation, as monthly averages (error bars show ±1 standard deviation; n=20–26). Data from Cain and others (2022).

Table 1. Concentrations of fine particles in surface sediments and major and minor inorganic elements for samples collected from Palo Alto site, California, 2020. Data from Cain and others (2022).

[Units for aluminum (Al), iron (Fe), fine sediment, and total organic carbon (TOC) are percentage of dry weight. Fine sediment is operationally determined as ≤100 micrometer grain size. Metals concentrations for the monthly samples are reported as the mean ±1 standard deviation (std) for replicate subsamples (number of samples [n]=2), except mercury (Hg) and selenium (Se), which are single measurements (n=1). Units are milligram per kilogram (mg/kg) dry weight, except Al and Fe. Means for monthly samples were summarized and reported as the annual mean ± the standard error (SEM) (n=6 or 8). All concentrations are based on near-total extracts, except for silver (Ag), which is based on partial extraction, mercury (Hg), and selenium (Se) (see section, "Methods"). Other elements: Cr, chromium; Cu, copper; Ni, nickel; Zn, zinc. Abbreviations: nd, no data; %, percent; TOC, total organic content; SEM, standard error of mean]

Date	Fine sediment (%)	Ag	Al (%)	Cr	Cu	Fe (%)	Hg	Ni	Se	Zn	TOC (%)
01/18/2020	71	0.25±0.007	2.7±0.03	91±0.4	33±0.1	3.6±0.01	0.45	79±0.2	0.37	111±0.4	1.17±0.04
02/17/2020	84	0.25±0.011	3.3±0.14	106±1	36±0.7	4.1±0.08	0.26	92±0.8	0.35	119±1.3	1.55±0.02
03/16/2020	82	0.21±0.010	3.2±0.07	103±1	38±0.6	4.1±0.04	nd	92±1.1	nd	124±3.9	1.38±0.03
05/13/2020	90	0.26±0.007	3.1±0.07	103±0.1	37±0.6	3.9±0.01	0.30	87±1.2	0.35	117±1.4	1.32±0.01
06/23/2020	77	0.22±0.006	2.8±0.03	94±0.1	35±0.1	3.6±0.01	0.29	83±0.7	0.32	113±0.1	1.19±0.04
09/19/2020	77	0.21±0.002	2.5±0.09	86±3	32±0.1	3.4±0.003	0.33	77±1.1	0.30	103±5.0	1.00±0
10/23/2020	68	0.18±0.012	2.2±0.01	83±1	29±0.2	3.1±0.02	nd	68±0.8	nd	92±0.6	1.16±0.22
12/11/2020	90	0.28±0.012	3.0±0.04	100±3	34±0.04	3.8±0.02	0.32	83±1.4	0.34	112±3.5	1.32±0.02
Annual mean	80	0.23	2.9	96	34	3.7	0.33	83	0.34	111	1.26
SEM	3	0.01	0.1	3	1	0.1	0.03	3	0.01	4	0.06

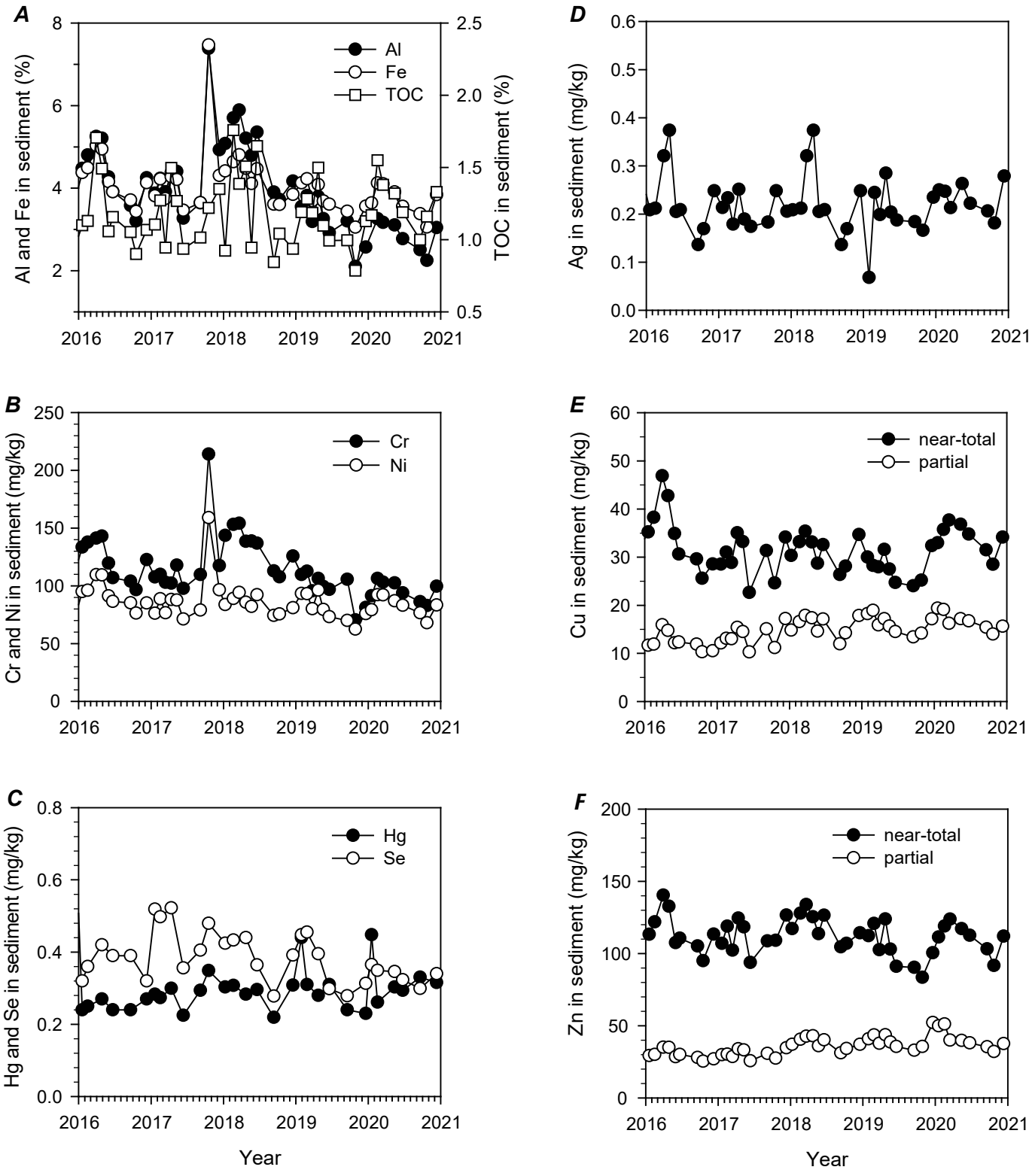

Figure 4. Graphs showing concentrations of metals and total organic carbon (TOC) in sediments at Palo Alto site, California, 2016–2020. *A*, Aluminum (Al), iron (Fe), and TOC. *B*, Chromium (Cr) and nickel (Ni). *C*, Mercury (Hg) and selenium (Se). *D*, Silver (Ag). *E*, Near-total and partially extracted copper (Cu). *F*, Near-total and partially extracted zinc (Zn). Data represent mean values. Other abbreviations: mg/kg, milligram per kilogram; %, percent.

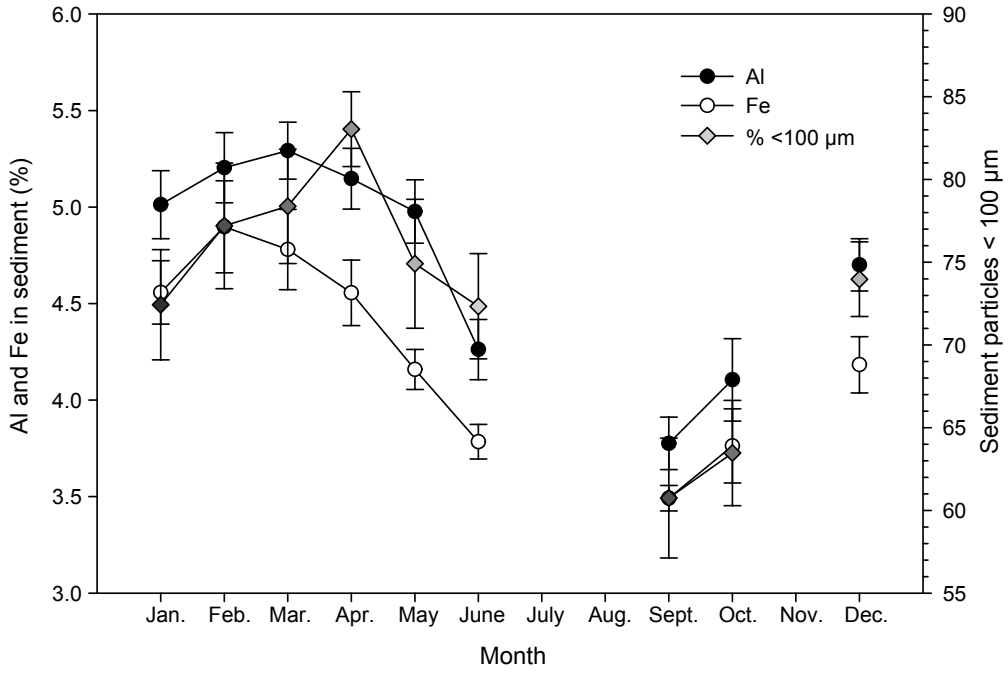

Figure 5. Graph showing general seasonal variations in aluminum (Al), iron (Fe), and percentage (%) of fine sediments (<100 micrometers [µm]) at Palo Alto site, California. Data are monthly mean of all samples collected from 1994 to 2020. Gaps in data indicate that samples were not collected in July, August, or November. Error bars show ±standard error of mean (SEM).

Sedimentary concentrations of all metals vary among years, and concentrations of some metals—notably silver and copper during the 1980s—have decreased (fig. 6). From 1994 to 2020, correlations between year and annual mean concentrations of iron (fig. 6*A*), silver (fig. 6*D*), copper (near total and partial extractable) (fig. 6*E*), and zinc (near total and partial extractable) (fig. 6*F*) were significant (p<0.05) and negative, suggesting that the concentration of these metals had decreased. A weak correlation exists between TOC (not illustrated) and year (r=–0.40, p=0.04). However, the correlation is dependent on the lowest value in the dataset (2014). For aluminum (fig. 6*A*), chromium (fig. 6*B*), nickel (fig. 6*B*), mercury (fig. 6*C*), selenium (fig. 6*C*), and the percentage of fine particles (not shown), correlations with year were insignificant (p>0.05), which indicates the absence of a trend over that period.

The National Oceanic and Atmospheric Administration has developed two levels of chemical concentration to screen sediments for their probable toxicity (Long and others, 1995). The effects range low (ERL) is defined as the concentration below which the incidence of adverse effects on sensitive species is rare (<10 percent). Adverse effects are expected to occasionally occur at concentrations between the ERL and the effects range median (ERM). Concentrations of several metals considered in this study are between the ERL and ERM.

Annual concentrations of chromium in surface sediment ranged from 96 to 163 milligrams per kilogram (mg/kg) and nickel concentrations ranged from 72 to 100 mg/kg (fig. 6*B*). In 2020, concentrations were 96±3 and 83±3 mg/kg for chromium and nickel, respectively (table 1). Although concentrations of both elements exceed their ERLs (81 and 21 mg/kg, respectively, for chromium and nickel), they likely reflect nonanthropogenic inputs from local watersheds that host geologic formations that are naturally enriched in both metals (Hornberger and others, 1999; Topping and Kuwabara, 2003).

Mercury concentrations in sediment from the Palo Alto site typically range from 0.24 (10th percentile) to 0.33 (90th percentile) mg/kg and have occasionally exceeded 0.40 mg/kg (in 2004 and 2015). In 2020, mercury averaged 0.33±0.03 mg/kg (fig. 6*C*; table 1), with the minimum in February (0.26 mg/kg) and the maximum in January (0.45 mg/kg). Sedimentary concentrations of total mercury in Palo Alto sediments typically range from the ERL (0.15 mg/kg) to the ERM (0.71 mg/kg).

Sedimentary selenium ranged from 0.24 and 0.79 mg/kg for 1994–2020 (fig. 6*C*). The annual mean selenium concentration in 2020 was 0.34±0.01 mg/kg, similar to the concentrations in 2018 and 2019.

The annual mean silver concentration at the Palo Alto site was 0.23±0.01 mg/kg in 2020. Silver concentrations were much higher when samples were first collected in the latter half of the 1970s. From 1977 to 1981, silver exceeded the ERL (1.0 mg/kg) (fig. 6*D*), then it decreased substantially during the 1980s to concentrations well below the ERL. Since 1994, silver concentrations ranged from 0.20 to 0.49 mg/kg and have decreased slightly, but they still exceeded what is considered the regional background concentration of 0.10 mg/kg (Hornberger and others, 2000).

Copper concentration (near total) has exceeded the ERL on an annual basis for most of the record (fig. 6*E*). However, concentrations decreased with time and have decreased to less than the ERL in some years. In 2020, the annual mean copper concentration was at the ERL (34 mg/kg) (table 1).

Zinc concentrations on an annual basis were less than the zinc ERL (150 mg/kg) for the entire record (fig. 6*F*; table 1). Exceedances of near-total zinc within some years typically occurred during the winter season (for example, in 2006 and 2015; fig. 6*F*). In 2020, the annual mean zinc concentration was 111±4 mg/kg, with a maximum concentration of 124±3.9 mg/kg in March (table 1).

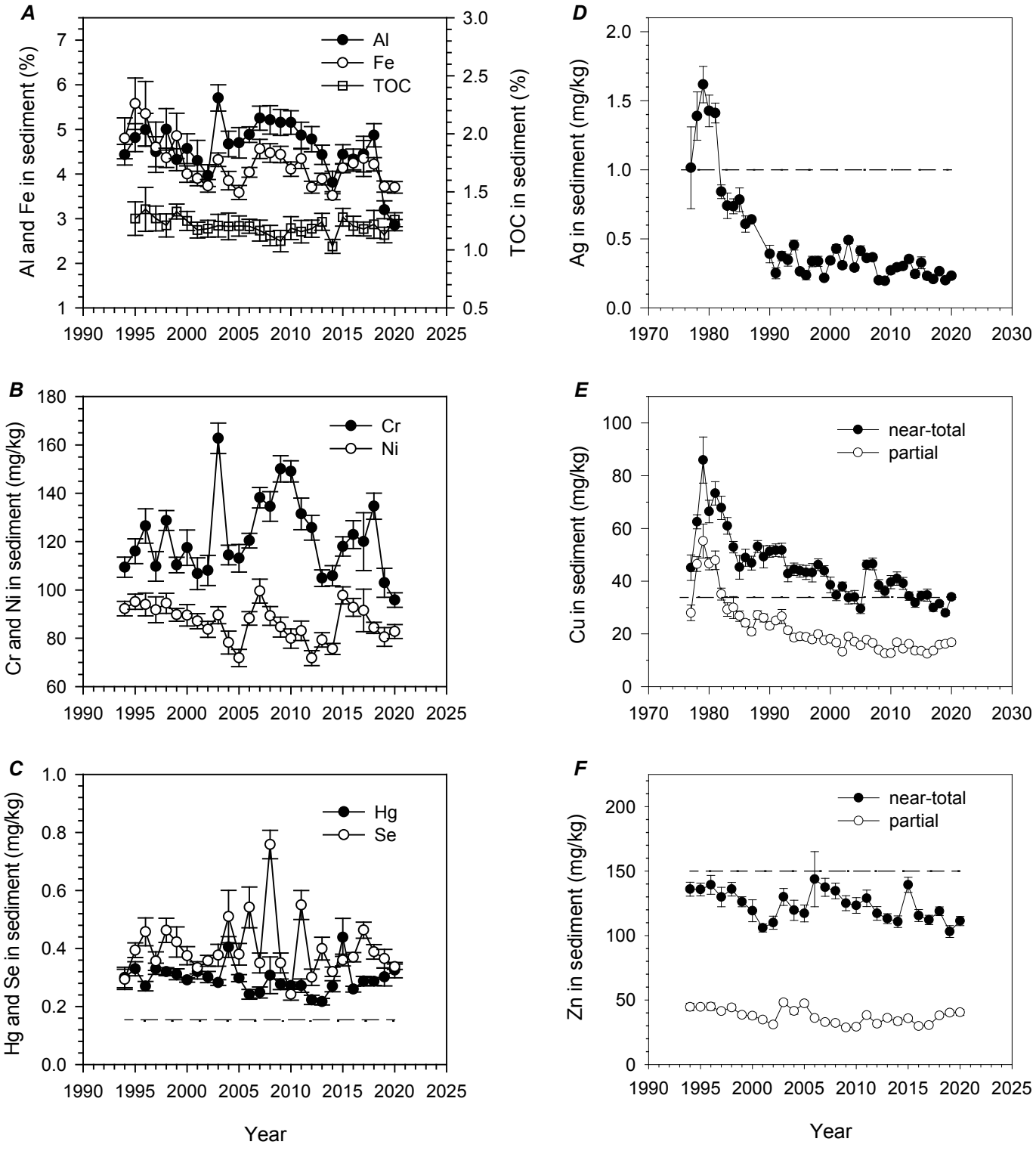

Figure 6. Graphs showing annual concentrations of metals and total organic carbon (TOC) in sediments at Palo Alto site, California. *A*, Aluminum (Al), iron (Fe), and TOC. *B*, Chromium (Cr) and nickel (Ni); ERL values for chromium (81 mg/kg) and nickel (20.9 mg/kg) not shown. *C*, Mercury (Hg) and selenium (Se). *D*, Silver (Ag). *E*, Near-total and partially extracted copper (Cu). *F*, Near-total and partially extracted zinc (Zn). Data are from 1994 to 2020 (*A*, *B*, *C*, *F*) or from 1977 to 2020 (*D*, *E*). Values are grand mean of monthly means of samples for given year. Error bars show ±standard error of those means (SEM). Dashed lines in *C*, *D*, *E*, and *F* represent effects range low (ERL) values, which show concentrations below which incidence of adverse effects on biota is expected to be low (<10 percent). Other abbreviations: mg/kg, milligram per kilogram; %, percent.

Clam Tissue

Metal concentrations in the soft tissues of *L. petalum* display a consistent seasonal pattern characterized by fall-winter maxima and spring-summer minima with the amplitude of the cycle fluctuating from year to year (fig.7). This variation in metal concentration reflects a combination of the metal accumulation from water and food, and the diluting and concentrating effects of gaining and losing tissue mass associated with annual growth and reproductive cycles (Cain and Luoma, 1990) represented by the CI. These CI values typically increase through winter to a maximum

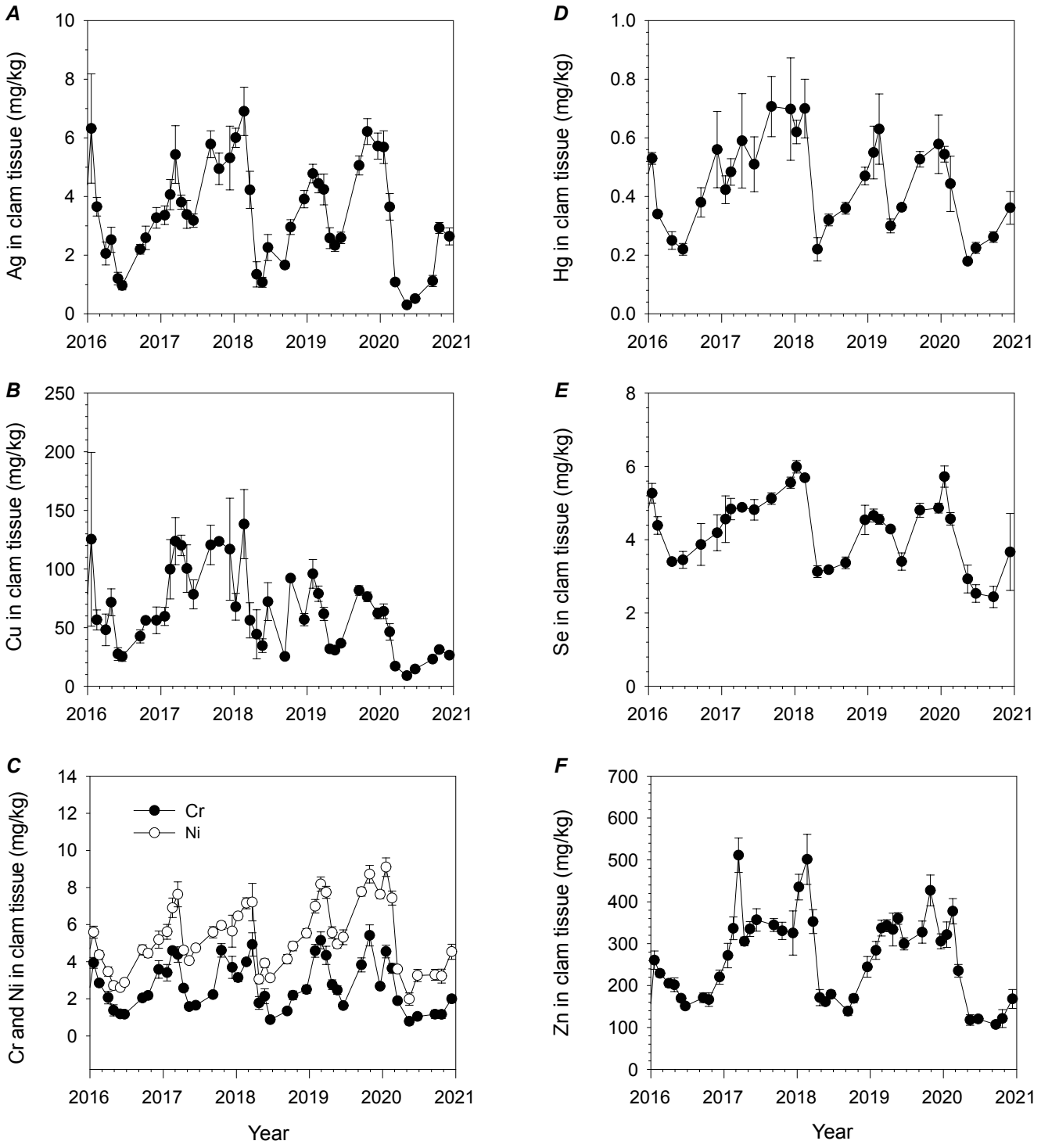

Figure 7. Graphs showing metal concentrations in soft tissues of clam *Limecola petalum*, in milligrams per kilogram (mg/kg), at Palo Alto site, California, 2016–2020. *A*, Silver (Ag). *B*, Copper (Cu). *C*, Chromium (Cr) and nickel (Ni). *D*, Mercury (Hg). *E*, Selenium (Se). *F*, Zinc (Zn). Values represent mean concentration for sample collected on given date. Error bars show ±standard error of those means (SEM).

in the spring (pre-spawning period), then taper off through summer-fall (fig. 8), a seasonal pattern that is opposite to that displayed by metal concentrations. The coupling between metal concentrations in soft tissue and recurring cycles of growth and reproduction can be illustrated, for example, by the seasonal patterns in copper and silver and CI (fig. 8). From 1994 to 2020, both metals correlated strongly with CI (for Cu, r=−0.96, p<0.01; for Ag, r=−0.95, p<0.01).

Exposures to copper and silver at the Palo Alto site are of special interest because of the high tissue concentrations at this site in the past (fig. 9*A*; appendix 6). From 1977 to 1993, the ranges in annual concentrations of copper and silver were 24 to 282 and 3.3 to 113 mg/kg, respectively. Since 1994, the ranges in mean annual concentrations of copper and silver were 26 to 105 and 1.8 to 7.6 mg/kg, respectively. Since 1994, median concentrations for copper and silver are 32 and 2.9 mg/kg, respectively. In 2020, the annual mean concentrations of copper and silver were 29±6 and 2.2±0.65 mg/kg, respectively (Table 2).

Tissue concentrations of other trace metals have been relatively stable. Since 1994, the maximum/minimum ratios for concentrations of chromium (fig. 9*B*), nickel (fig. 9*B*), mercury (fig. 9*C*), selenium (fig. 9*C*), and zinc (fig. 9*D*) are about 2. Concentrations measured in 2020 were not atypical of concentrations in previous years, although consistently lower than in 2019. In 2020, the annual mean concentrations of chromium and nickel were 2.0±0.48 and 4.6±0.86 mg/kg, respectively (table 2). Mercury was 0.34±0.06 mg/kg, selenium was 3.6±0.53 mg/kg, and zinc was 196±37 mg/kg (table 2).

From 1994 to 2020, tissue concentrations of silver, chromium, mercury, and zinc were correlated with year. Correlations were negative for silver (r=−0.41), chromium (r=−0.44), and zinc (r=−0.46), and positive for mercury (r=0.46). Multiple linear regression was used to examine some of the potential underlying variables affecting the temporal trends in these metals. Independent variables included sedimentary metal, CI, and year. Year is a surrogate variable for other unidentified variables. Data used for the analysis were the annual means. Variables were transformed, as necessary, to fit the data to the normal distribution.

Results showed that the CI was predictive of the concentrations of silver (multiple R^2=0.41) and zinc (multiple R^2=0.50). Year and sedimentary metals were not significant predictors. For these two metals, the modest downward trend in tissue concentrations appeared to be related to the CI. Silver and zinc concentrations in *L. petalum* decreased as the condition index increased.

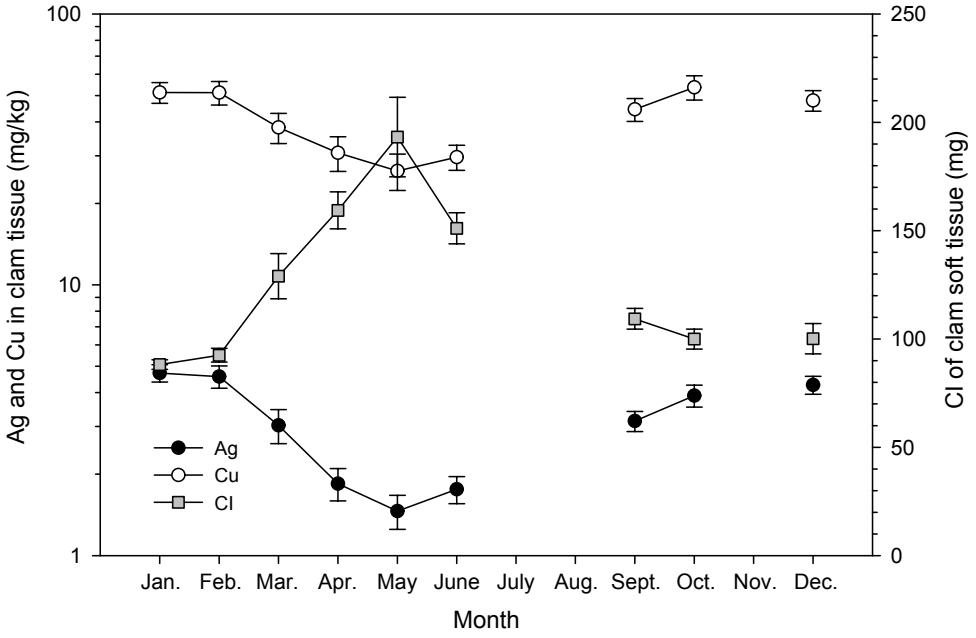

Figure 8. Graph showing seasonal patterns in condition index (CI) and concentrations of silver (Ag) and copper (Cu) of clam *Limecola petalum* at Palo Alto site, California. Condition index is defined as tissue weight (in milligrams [mg]) of soft tissues for an individual clam that has shell length of 25 millimeters (mm). Ag and Cu concentrations in milligrams per kilogram (mg/kg). Data are grand mean of monthly means from 1994 to 2020. Error bars show ±standard error of those means (SEM). Samples typically were not collected in July, August, or November, and thus were omitted.

The MLR model with year, sedimentary chromium, and CI as independent variables explained little of the variance of chromium in *L. petalum* (multiple R^2=0.26, p<0.02). However, more variance was explained by CI (beta=−0.32) than by sedimentary chromium (beta=0.27) or year (beta=−0.24), suggesting that the slight downward trend in chromium is more likely related to the CI than the other two variables.

The MLR model for mercury was significant (R^2=0.33, p=0.02) with year as the only significant predictor (beta=0.65, p=0.003). The result suggests that mercury concentration increased despite the countervailing effects of CI observed for other metals (mercury and CI are not correlated in the dataset [r=−0.01]). The positive correlation between year and mercury (r=0.46, p=0.02) is driven by the relatively high concentrations in 2017 and 2019.

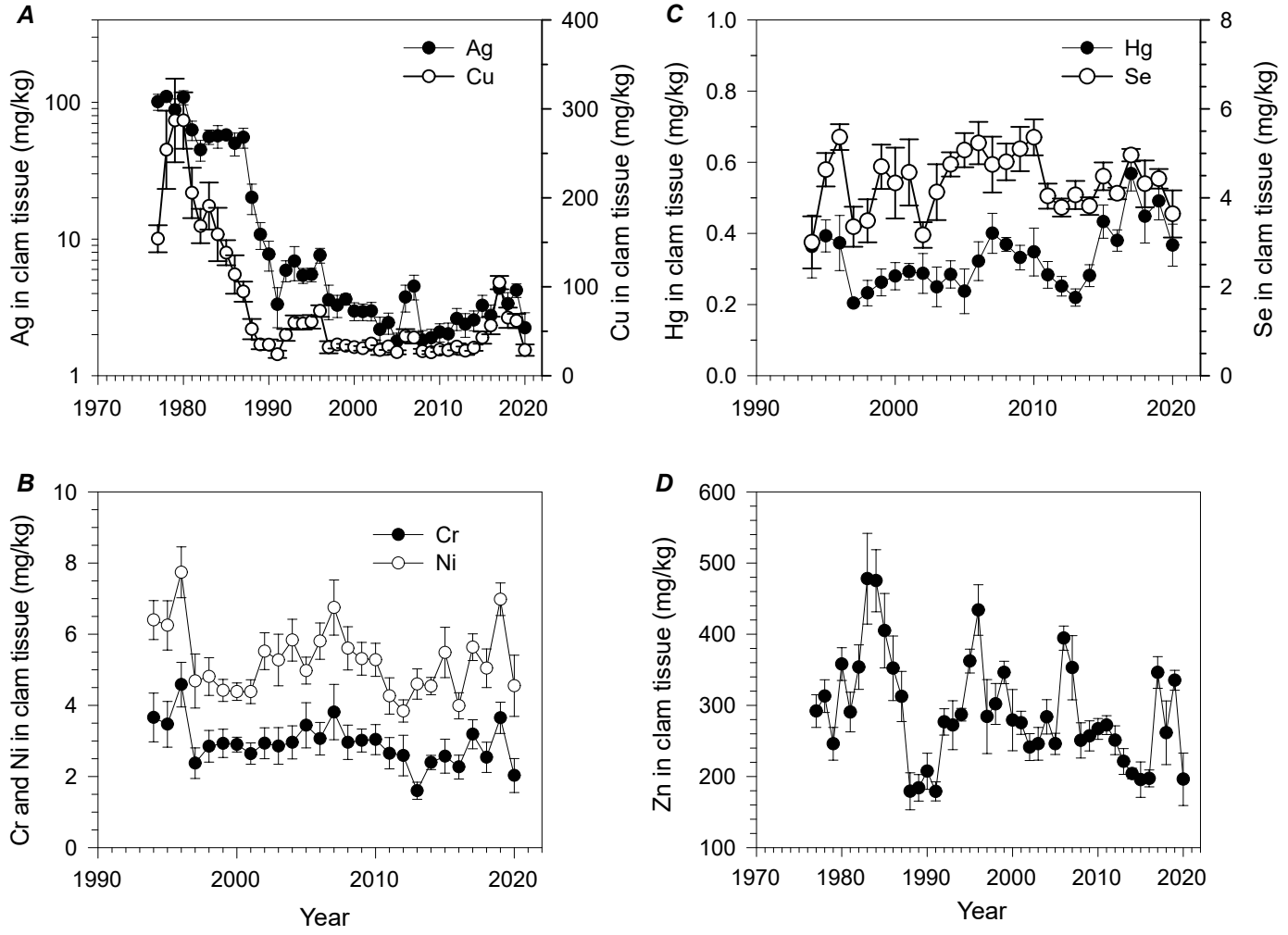

Figure 9. Graphs showing metal concentrations in clam *Limecola petalum,* in milligrams per kilogram (mg/kg), at Palo Alto site, California. *A*, Copper (Cu) and silver (Ag). *B*, Chromium (Cr) and nickel (Ni). *C*, Mercury (Hg) and selenium (Se). *D*, Zinc (Zn). Data are from 1977 to 2020 (*A*, *D*) or from 1994 to 2020 (*B*, *C*). Values are annual (grand) mean. Error bars show ±standard error of those means (SEM).

Table 2. Concentrations of trace metals in, and the condition index of, clam *Limecola petalum* at Palo Alto site, California, 2020.

[Units for elemental concentrations are milligrams per kilogram (mg/kg) soft tissue dry weight; units for condition index (CI) are milligrams. Condition index is defined as soft tissue weight of clam of 25-millimeter shell length. All concentrations are based on near-total extracts. Monthly data are reported as mean ±standard deviation for replicate composites (number of samples [n]=6–11), except for selenium (Se) and mercury (Hg) (n=2–3); means for monthly samples were summarized and reported as annual (grand) mean ±standard error (SEM) (n=6 or 8). Other elements: Ag, silver; Cr, chromium; Cu, copper; Ni, nickel; Zn, zinc. Abbreviations: CI, conditional index; nd, no data; SEM, standard error of mean]

Date	Ag	Cr	Cu	Hg	Ni	Se	Zn	CI
01/18/2020	5.7±1.8	4.5±1.1	64±20	0.54±0.05	9.1±1.6	5.7±0.5	321±96	64
02/17/2020	3.6±1.5	3.6±0.9	46±23	0.44±0.16	7.4±1.3	4.6±0.3	377±100	89
03/16/2020	1.1±0.2	1.9±0.3	17±3	nd	3.6±0.4	nd	236±40	180
05/13/2020	0.3±0.1	0.8±0.5	9±3	0.18±0.02	2.0±0.9	2.9±0.4	118±33	465
06/23/2020	0.5±0.2	1.0±0.5	15±3	0.22±0.03	3.3±1.0	2.5±0.4	120±12	162
09/19/2020	1.1±0.6	1.2±0.7	23±6	0.26±0.03	3.3±0.9	2.4±0.5	107±23	142
10/22/2020	2.9±0.5	1.2±0.5	31±5	nd	3.2±0.9	nd	121±52	137
12/11/2020	2.6±0.9	2.0±0.6	26±3	0.36±0.10	4.5±1.2	3.7±1.8	168±68	94
Annual mean	2.2	2.0	29	0.34	4.6	3.6	196	167
SEM	0.65	0.48	6	0.06	0.86	0.53	37	45

Reproduction of *Limecola petalum*

As previously reported, reproductive output in *L. petalum* appeared to be impaired by high tissue concentrations of silver during the early part of the record (Hornberger and others, 1999; Shouse and others, 2003). The time series of reproductive activity shows that following the decrease in silver during the 1980s, reproductive output increased, and it has remained at relatively high levels. Since 1998, a high percentage of the animals were reproductively active at any given time, and they did not stay reproductively inactive for longer than a month or two. Moreover, normal seasonal cycling of reproduction—beginning in the fall and continuing through the following spring—is evident (figs. 10, 11, appendix 7).

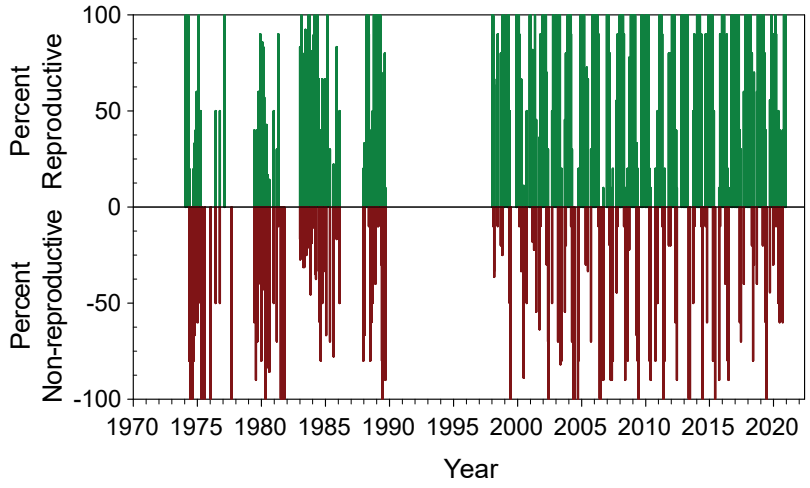

Figure 10. Graph showing reproductive activity of clam *Limecola petalum* at Palo Alto site, California, 1974–2020. Values are percentages (%) of individuals that either were in various stages of reproduction (reproductive shown as positive values) or were reproductively inactive (nonreproductive shown as negative values).

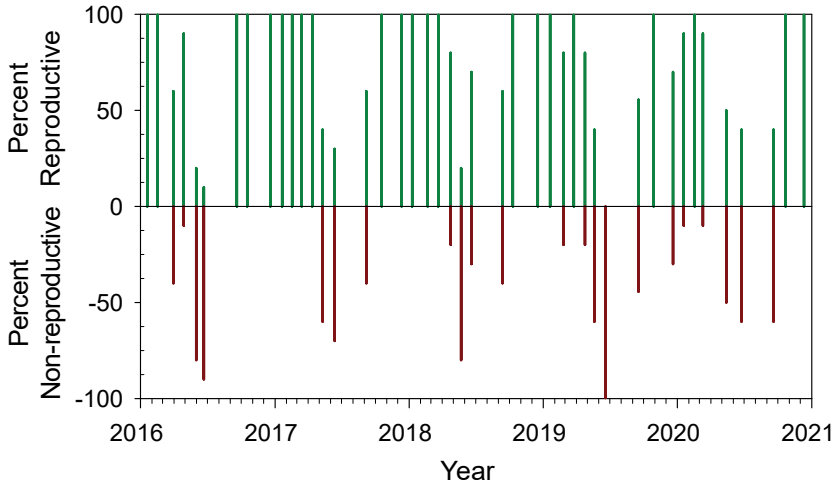

Figure 11. Graph showing reproductive activity of clam *Limecola petalum at* Palo Alto, California, 2016–2020. Values are percentages (%) of individuals that either were in various stages of reproduction (reproductive shown as positive values) or were reproductively inactive (nonreproductive shown as negative values).

Benthic Community

Estimates of benthic species diversity and total animal abundance are fundamental metrics that are used to assess environmental stress on biological communities. Species diversity at the Palo Alto site, as estimated by a time series of number of species, was at a minimum in 1998 (with the exceptions of 2008, discussed below), trended upward through 2012, and has shown a slight decrease since its peak in 2012 (fig. 12). Total animal abundance has varied significantly during the sampling period (fig. 13). The difficulty with these types of metrics is that they do not consider the possibility that one species can take the place of another, or that high abundance is based on one species. The community structure and function may change as a result of shifts in species composition, depending on the characteristics of a newly introduced or newly dominant species. The details of changes in species composition are important because they may reflect the relative ability of species to accommodate environmental stress and redistribute site resources. In general, the species composition at the study site has changed little since 1998, although seasonal eruptions of several species have occurred in some years.

Three common bivalves (*Limecola petalum*, *Mya arenaria*, and *Gemma gemma*) have not shown any consistent trend over the 46-year period from 1974 to 2020 (figs. 14–16). Species abundance has shown significant seasonal and interannual variability for all species found at the Palo Alto site. The three common bivalves illustrate this variability well. *G. gemma* has been particularly volatile since 2005; its abundance decreased to near zero in late fall 2007 and subsequently took 3 years to recover to previous average densities, which have continued through the present (2020).

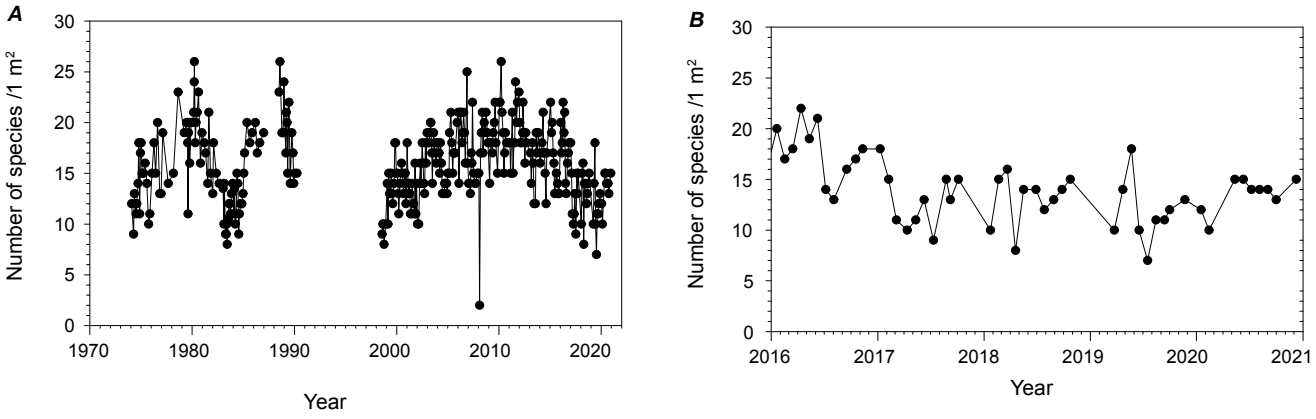

Figure 12. Graphs showing total number of species present at Palo Alto site, California, (*A*) 1974–2020 and (*B*) 2016–2020. Sampling site was 1 square meter (m²). Samples were not collected in 1987 nor from 1991 to 1997.

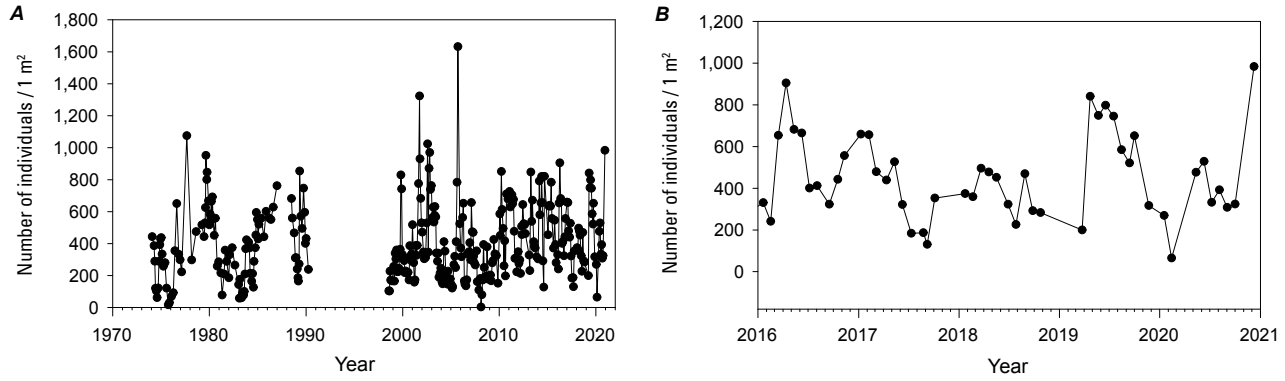

Figure 13. Graphs showing total average number of individuals present at Palo Alto site, California, (*A*) 1974–2020 and (*B*) 2016–2020. Sampling site was 1 square meter (m²). Samples were not collected in 1987 nor from 1991 to 1997.

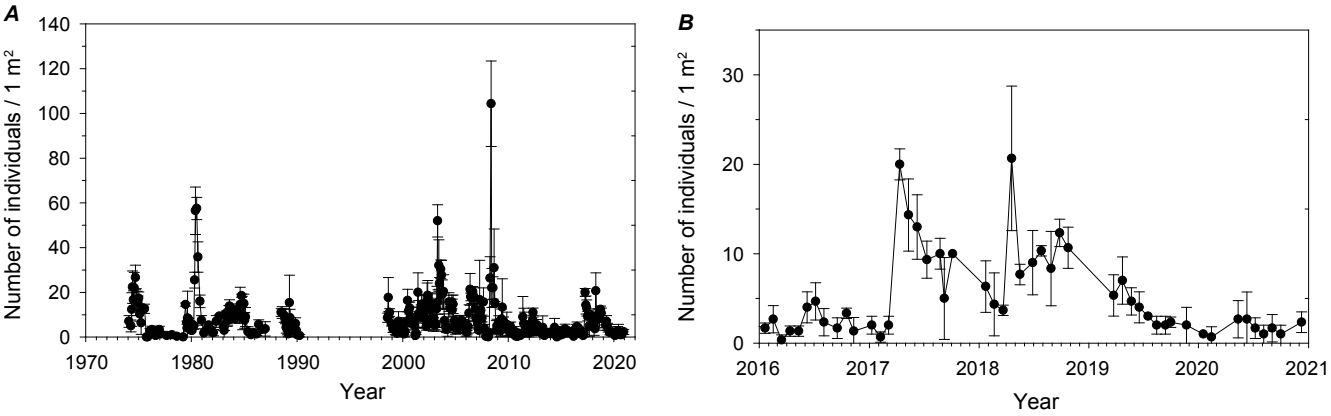

Figure 14. Graphs showing monthly average abundance of *Limecola petalum* at Palo Alto site, California, (*A*) 1974–2020 and (*B*) 2016–2020. Sampling site was 1 square meter (m²). Error bars represent ±standard deviation from three replicate samplings. Samples were not collected in 1987 nor from 1991 to 1997.

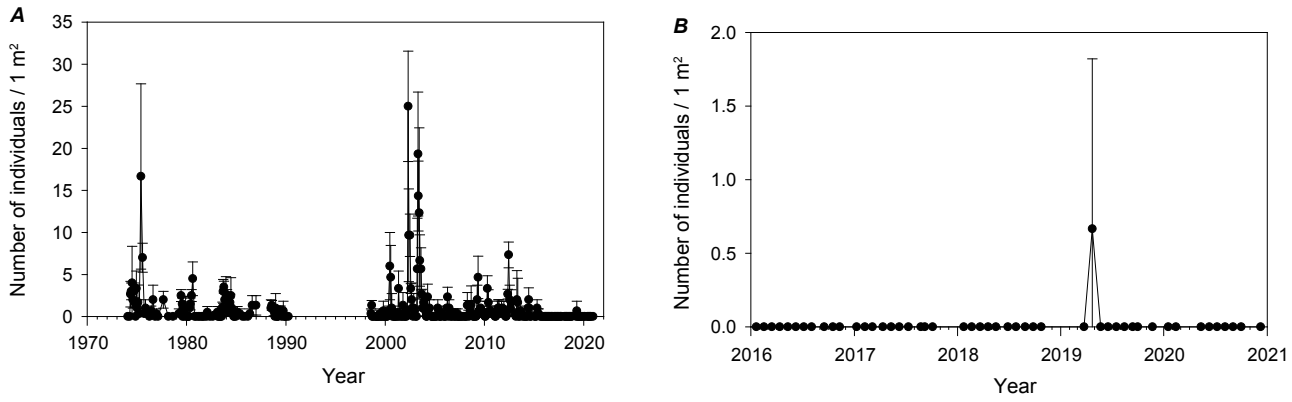

Figure 15. Graphs showing monthly average abundance of *Mya arenaria* at Palo Alto site, California, (*A*) 1974–2020 and (*B*) 2016–2020. Sampling site was 1 square meter (m²). Error bars represent ±standard deviation from three replicate samplings. Samples were not collected in 1987 nor from 1991 to 1997.

Six species have shown downward trends in their abundance since the 1970s. *Ampelisca abdita* is a small crustacean that lives above the surface of the mudflat in a tube built from selected sediment particles. *A. abdita* showed a general decrease in abundance (fig. 17) after 1998, and mostly low abundances persisted through the present (2020). *Streblospio benedicti* is a small polychaete worm that also builds a tube above the surface of the mudflat. *S. benedicti* abundance has decreased through the study years and, over the past 10 years, the species has maintained a seasonal pattern of increasing spring abundance followed by a fall-winter decrease (fig. 18). The abundance of the small burrowing crustacean *Grandidierella japonica*, a deposit feeder, became more seasonally consistent after 2000 (fig. 19), with particularly low abundances in 2006, 2007, and 2011. This species has shown a consistent seasonal peak in abundance in the fall since 1999, with the exception of 2011. *Alitta succinea*, a burrowing polychaete that feeds on surface deposits and scavenges for detrital food, showed large seasonal fluctuations in abundance throughout the study (fig. 20). Similar to other species, its abundance declined in 2011 and remains in low numbers today (2020).

Two species showed an increase in abundance within the time series. The first species, *Heteromastus filiformis* (fig. 21), is a burrowing, subsurface-deposit-feeding polychaete worm that lives deep in the sediment (usually 5–20 cm beneath the surface of the mudflat). Abundance increased sharply in 1985 and then partly receded in the late 1980s. Abundance remained higher than in the late 1970s until a decrease in 2008 and a slight increase after 2010 (fig. 21). Data from the 1980s

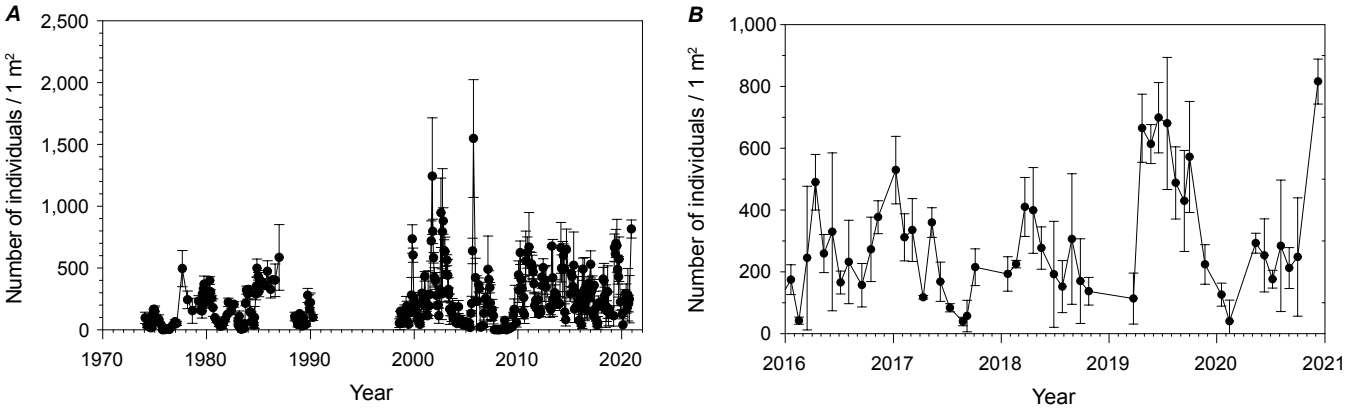

Figure 16. Graphs showing monthly average abundance of *Gemma gemma* at Palo Alto site, California, (*A*) 1974–2020 and (*B*) 2016–2020. Sampling site was 1 square meter (m^2). Error bars represent ±standard deviation from three replicate samplings. Samples were not collected in 1987 nor from 1991 to 1997.

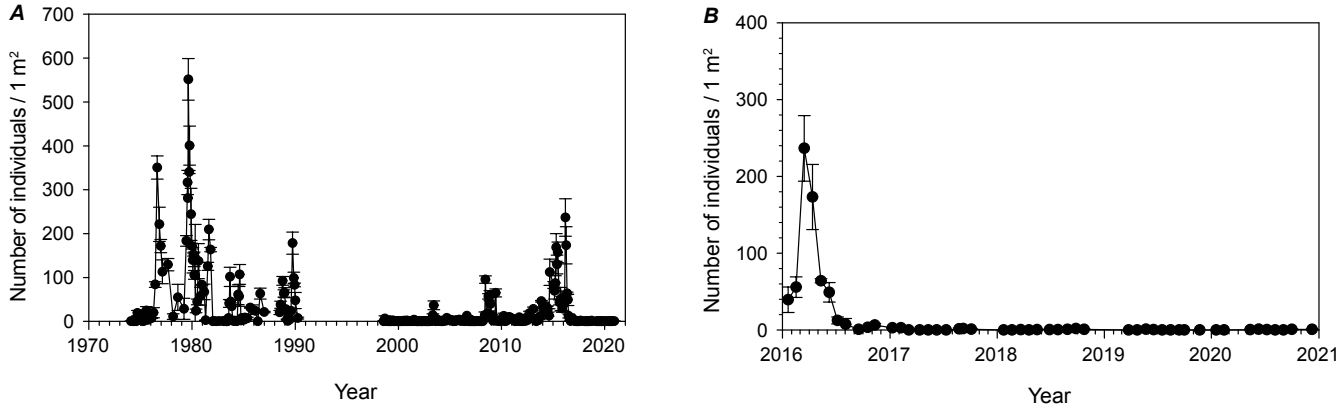

Figure 17. Graphs showing monthly average abundance of *Ampelisca abdita* at Palo Alto site, California, (*A*) 1974–2020 and (*B*) 2016–2020. Sampling site was 1 square meter (m^2). Error bars represent ±standard deviation from three replicate samplings. Samples were not collected in 1987 nor from 1991 to 1997.

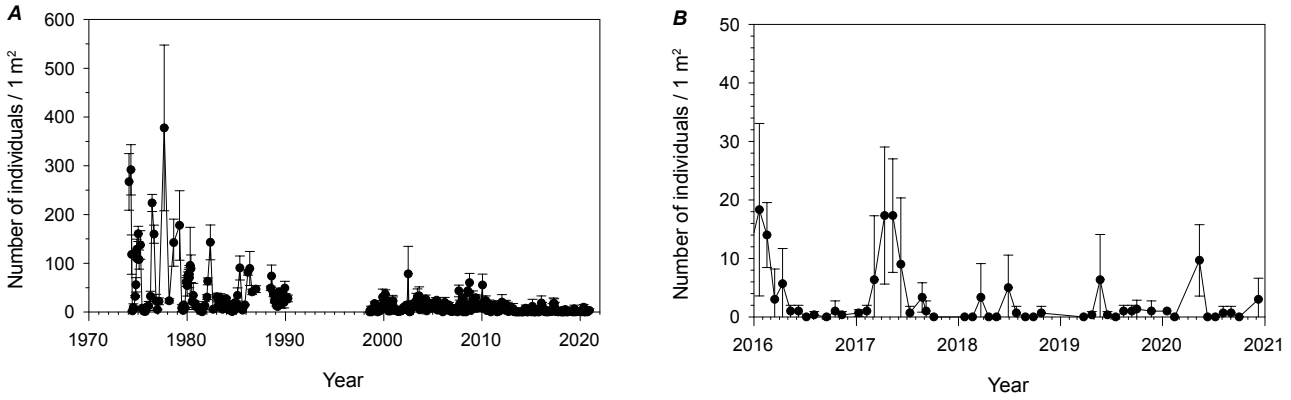

Figure 18. Graphs showing monthly average abundance of *Streblospio benedicti* at Palo Alto site, California, (*A*) 1974–2020 and (*B*) 2016–2020. Sampling site was 1 square meter (m^2). Error bars represent ±standard deviation from three replicate samplings. Samples were not collected in 1987 nor from 1991 to 1997.

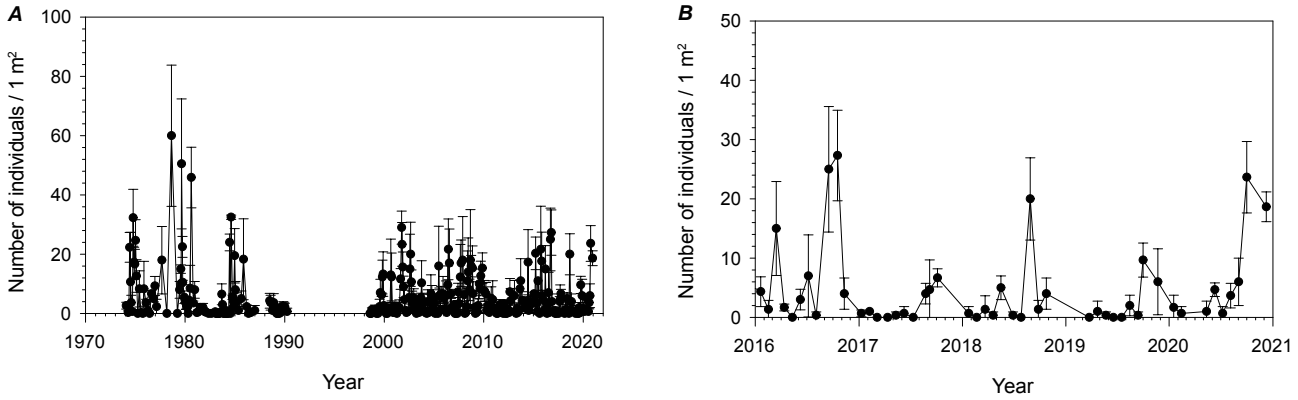

Figure 19. Graphs showing monthly average abundance of *Grandiderella japonica* at Palo Alto site, California, (*A*) 1974–2020 and (*B*) 2016–2020. Sampling site was 1 square meter (m^2). Error bars represent ±standard deviation from three replicate samplings. Samples were not collected in 1987 nor from 1991 to 1997.

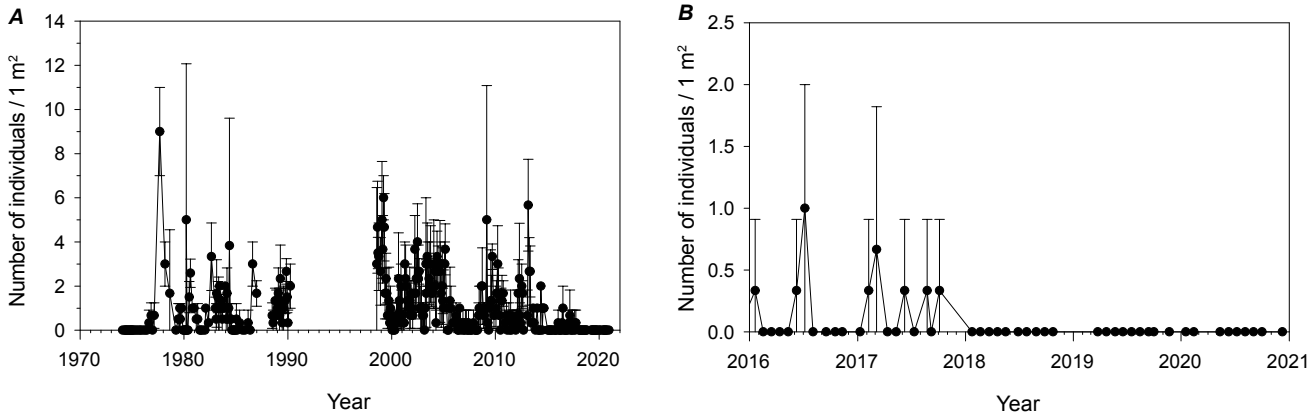

Figure 20. Graphs showing monthly average abundance of *Alitta succinea* (formerly *Neanthes succinea*) at Palo Alto site, California, (*A*) 1974–2020 and (*B*) 2016–2020. Sampling site was 1 square meter (m^2). Error bars represent ±standard deviation from three replicate samplings. Samples were not collected in 1987 nor from 1991 to 1997.

indicate that abundance for this species increases slowly, possibly because of their egg-laying mode of recruitment. The second species showing an increase was *Nippoleucon hinumensis*, a small, burrowing, surface-deposit-feeding crustacean, which appeared in the dataset in 1988 (fig. 22) following its introduction into the bay in 1986 (Cohen and Carlton, 1995).

A complete list of the benthic species found at the Palo Alto site in 2020 is shown in appendix 8. The benthic species name changes (as of 2020) for the species listed in appendix 8 are shown in appendix 9.

A sudden decrease in animal abundance was observed in February 2008 (fig. 13). Very few animals were observed at the Palo Alto site, and the mudflat community was evidently stressed by some event between the January and February sampling. Possible causes of the stress include sedimentation or freshwater inundation. A large storm occurred on January 25, 2008, with rainfall rates exceeding 0.5 centimeters per hour (cm/h) for more than one-half the day, including during the low-tide period. No obvious changes in the sediment surface were observed, but sediment changes can occur and be incorporated quickly in this tidal environment. Other possible causes of benthic community death or exodus include a toxic event or anoxia. Either of these events are unlikely to have occurred because *L. petalum* clams were present in the deep sediment in February 2008, and other taxa were found again in March. This would not happen with toxicity or anoxia. The timeline for recovery from anoxia can be estimated based on observations following an anoxic event at this site in 1975. Macroalgae were deposited on the mudflat surface and began to decay, and the resulting bacterial consumption of oxygen led to anoxia. The benthic community took many months

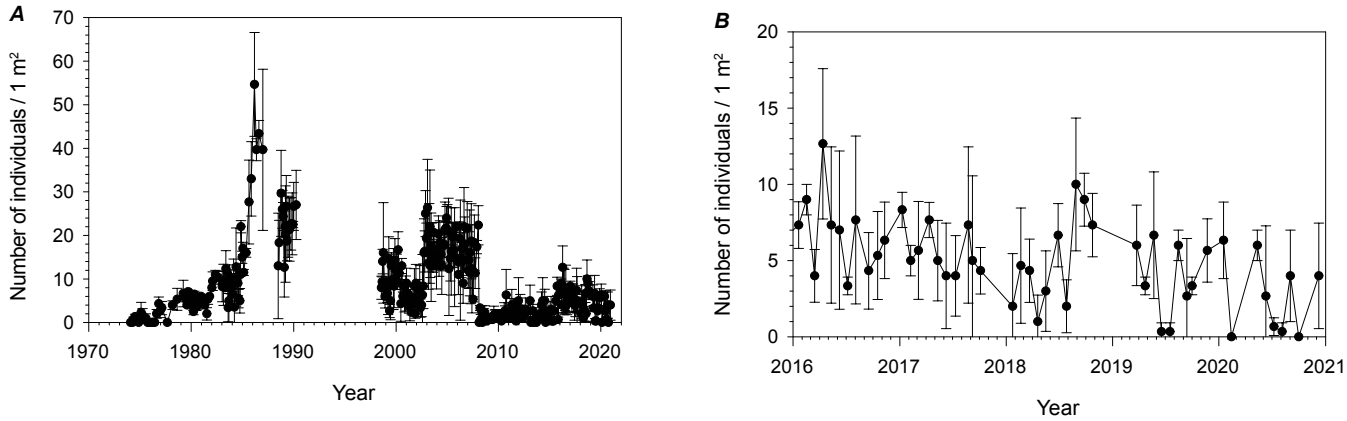

Figure 21. Graphs showing monthly average abundance of *Heteromastus filiformis* at Palo Alto site, California, (*A*) 1974–2020 and (*B*) 2016–2020. Sampling site was 1 square meter (m²). Error bars represent ±standard deviation from three replicate samplings. Samples were not collected in 1987 nor from 1991 to 1997.

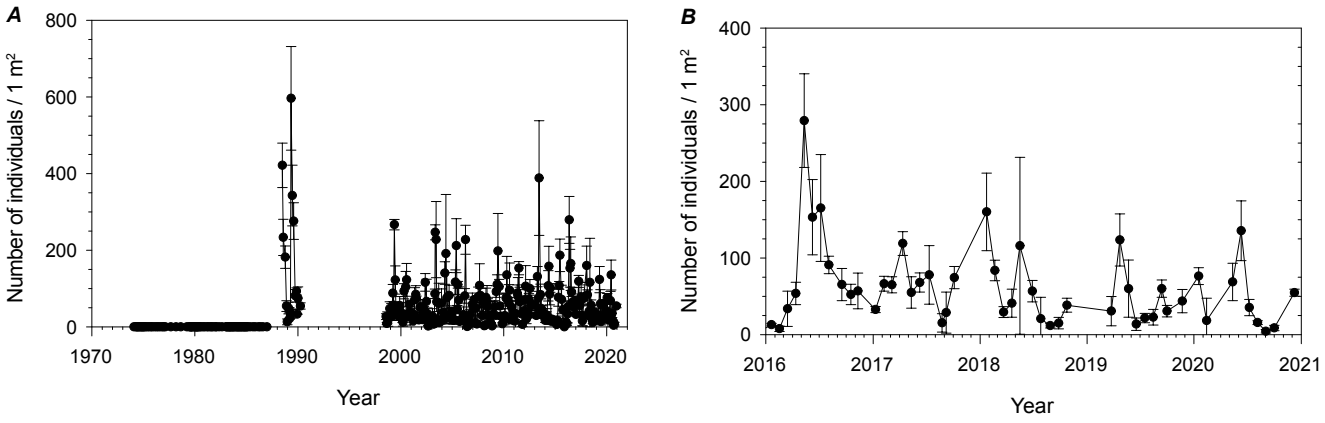

Figure 22. Graphs showing monthly average abundance of *Nippoleucon hinumensis* at Palo Alto site, California, (*A*) 1974–2020 and (*B*) 2016–2020. Sampling site was 1 square meter (m²). Error bars represent ±standard deviation from three replicate samplings. Samples were not collected in 1987 nor from 1991 to 1997.

to recover from this anoxic event (Nichols and Thompson, 1985a, 1985b). Animals that returned after the disturbance in 2008 include those species with pelagic larvae and mobile adults, as would be expected. Nonmobile brooders returned to the site in 2009, concurrent with an increase in abundance of the brooding clam *G. gemma* and the brooding polychaete *S. benedicti*. This trend continued into the present (2020), when brooder species were nearly one-half of the top 10 most abundant species, whereas oviparous and spawner species made up the rest.

Multivariate analyses of population data of the dominant species with environmental parameters did not reveal any relations, except with the concentration of silver and copper in the sediment and in the tissue of *L. petalum* (using data reported by David and others, 2002). Silver and copper concentration and abundance of species with the most susceptible mode of feeding and reproduction were compared over the period of the study. One susceptible species, the worm *H. filiformis*, increased in abundance with the decrease in silver and copper until 2008 (fig. 21). This was of interest because *H. filiformis* is a burrowing deposit feeder and, thus, has continuous internal and external tissue contact with the sediment. In addition, *H. filiformis* is one of the few species in the present community that reproduces exclusively by laying eggs in the sediment. The larvae hatch after 2 or 3 days and experience a very short planktonic period (2–3 days) before settling back to the mud as juvenile worms (Rasmussen, 1956). The short planktonic period limits the species' speed of expansion into new areas. We hypothesize that once a few individuals successfully arrived at the study site, *H. filiformis* increased in abundance because either the adult worms or the eggs found the environment agreeable. This species is not likely to move into an area quickly after an environmental stressor because of its mode of reproduction and short planktonic larval period. A large spike in *H. filiformis* abundance was observed in January 2008 owing to the settling of larvae, but these larvae did not survive the event that occurred before the February sampling. So far, the species has not returned in high numbers to the study site. The dynamics of recovery for this species will continue to be monitored closely.

Two species have shown the opposite trend of *H. filiformis*. The crustacean *A. abdita* (fig. 17) and the worm *S. benedicti* (fig. 18) have decreased in abundance coincident with the decrease in metals. These species have very similar life-history characteristics that make them less susceptible to high silver and copper concentrations in sediment. In contrast with the burrowing lifestyle of *H. filiformis*, both species live on the surface of the sediment in tubes that are built from sediment particles. Rather than feeding on the mud, they filter particles suspended in the water column or settled on the sediment surface. Instead of laying eggs in the mud, they brood their young and produce young that are capable of either swimming or settling upon hatching. These opportunistic characteristics make these species ideal for invading a disturbed or stressed environment; thus, they are capable of rapid increase in population size and distribution. Because of these characteristics, both species immediately responding to the near-empty community in February 2008 and subsequently decreasing in population is not surprising (figs. 17, 18). This abundance pattern is consistent with expectations for an opportunistic species, confirming both their tolerance to elevated metals and their inability to out-compete less opportunistic diverse communities in nonstressed conditions.

Other species share the characteristics highlighted in our discussion of *H. filiformis*, *S. benedicti*, and *A. abdita*. The species with similar characteristics have been combined into plots that examine the percentage of abundance represented by each feeding and reproductive mode (figs. 23–26). Each characteristic reproductive and feeding mode are shown as average percentages for August (figs. 23–26) because natural spatial variability (that is, the large standard deviations around the monthly means) and seasonal variability of invertebrate abundance can be quite large. To interpret these plots, the life-history characteristics must first be examined to determine if some mechanism exists by which this organism could be responding to a decrease in silver or copper in the environment. Silver, but probably not copper, is likely to have adversely affected reproduction of all animals (Hornberger and others, 2000). If species with pelagic larvae were transported into the area, they did not survive to dominate the community. Species having both oviparous and mixed (that is, species capable of oviparity and brooding) reproductive modes (Ahn and others, 1995; Hornberger and others, 2000) are worth examining in more detail. The gradual increase in abundance of this group through 1983 occurred concurrently with the gradual reduction of metals in the environment during that time. In the present environment, with much lower metal concentrations, these species respond to a different variety of stresses, and the percentage of brooding and oviparous individuals in the community reflects those stresses (figs. 23, 24). Although the percentage is variable, the number of brooders plus oviparous individuals has never been as high as it was in the early 1970s. We interpret this as reflecting the general health of the benthic environment. In a similar manner, we can examine the feeding modes of most of the individuals (figs. 25, 26). High silver and (or) copper concentrations in the sediment are unlikely to be healthy for species that ingest sediment in order to consume the interstitial and attached carbon; thus, species that consume particles from the water column can be reasonably expected to be more protected from the contaminants in the sediment. Filter-feeding species are usually the dominant group throughout the dataset, and the subsurface-deposit feeders are the group that shows the largest increase in dominance after the 1970s. This is consistent with the conceptual model posed in this report.

The change in function of the benthic community over time can be examined by ranking the top 10 species by abundance and plotting the log (n+1) of mean abundance against the rank of each species (Whittaker, 1965). The graph for 2016 to 2020 (fig. 27) is indicative of a healthy

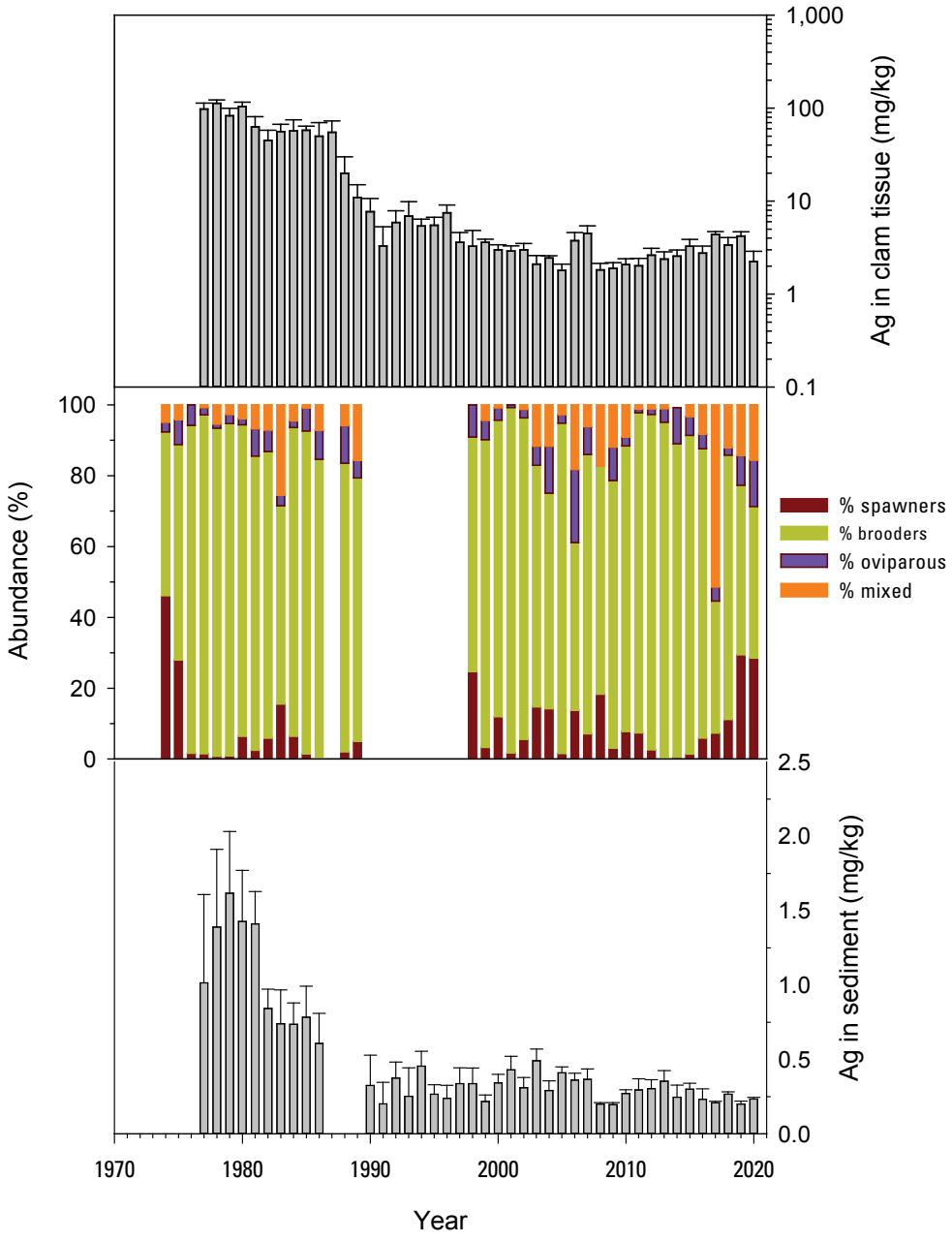

Figure 23. Graphs showing reproductive-mode annual abundances for top-10-ranked species (middle), as well as silver (Ag) concentrations in clam *Limecola petalum* (top) and in sediment (bottom), at Palo Alto site, California, 1974–2020 (samples were not collected from 1987 to 1989). Concentrations are grand mean ±standard error, in milligrams per kilogram (mg/kg). Abundance data (in percent [%]) for each year are from August of that year (samples were not collected in 1987 nor from 1991 to 1997). Reproductive modes: brooder, broods young and release juveniles as fully functional "miniature adults;" mixed, capable of ovipary and brooding; oviparous, lays eggs in or on sediment; spawner, releases gametes into water column and juveniles settle out of plankton onto sediment surface after growth in plankton.

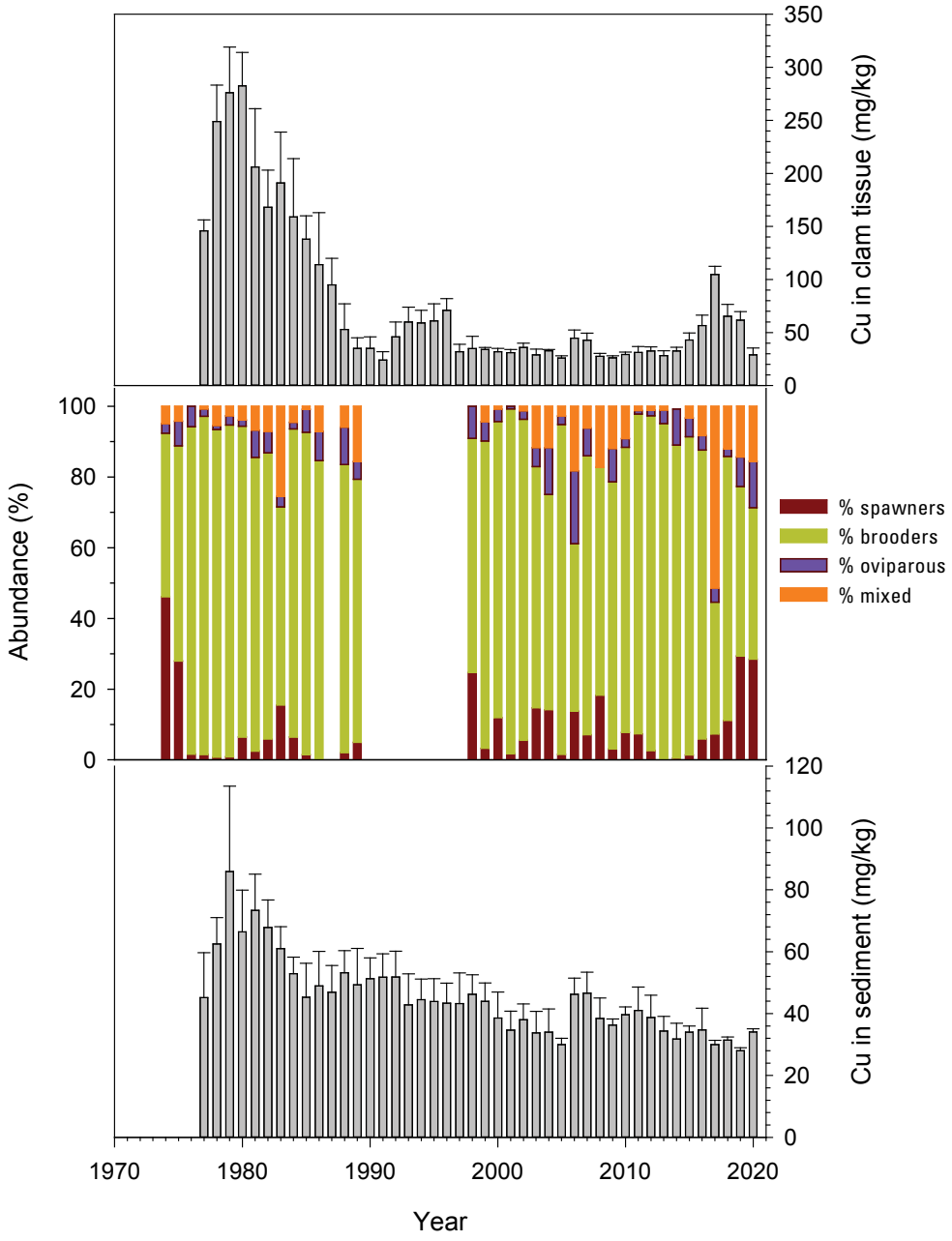

Figure 24. Graphs showing reproductive-mode annual abundances for top-10-ranked species (middle), as well as copper (Cu) concentrations in clam *Limecola petalum* (top) and in sediment (bottom), at Palo Alto site, California, 1974–2020. Concentrations are grand mean ±standard error, in milligrams per kilogram (mg/kg). Abundance data (in percent [%]) for each year are from August of that year (samples were not collected in 1987 nor from 1991 to 1997). Reproductive modes: brooder, broods young and release juveniles as fully functional "miniature adults;" mixed, capable of ovipary and brooding; oviparous, lays eggs in or on sediment; spawner, releases gametes into water column and juveniles settle out of plankton onto sediment surface after growth in plankton.

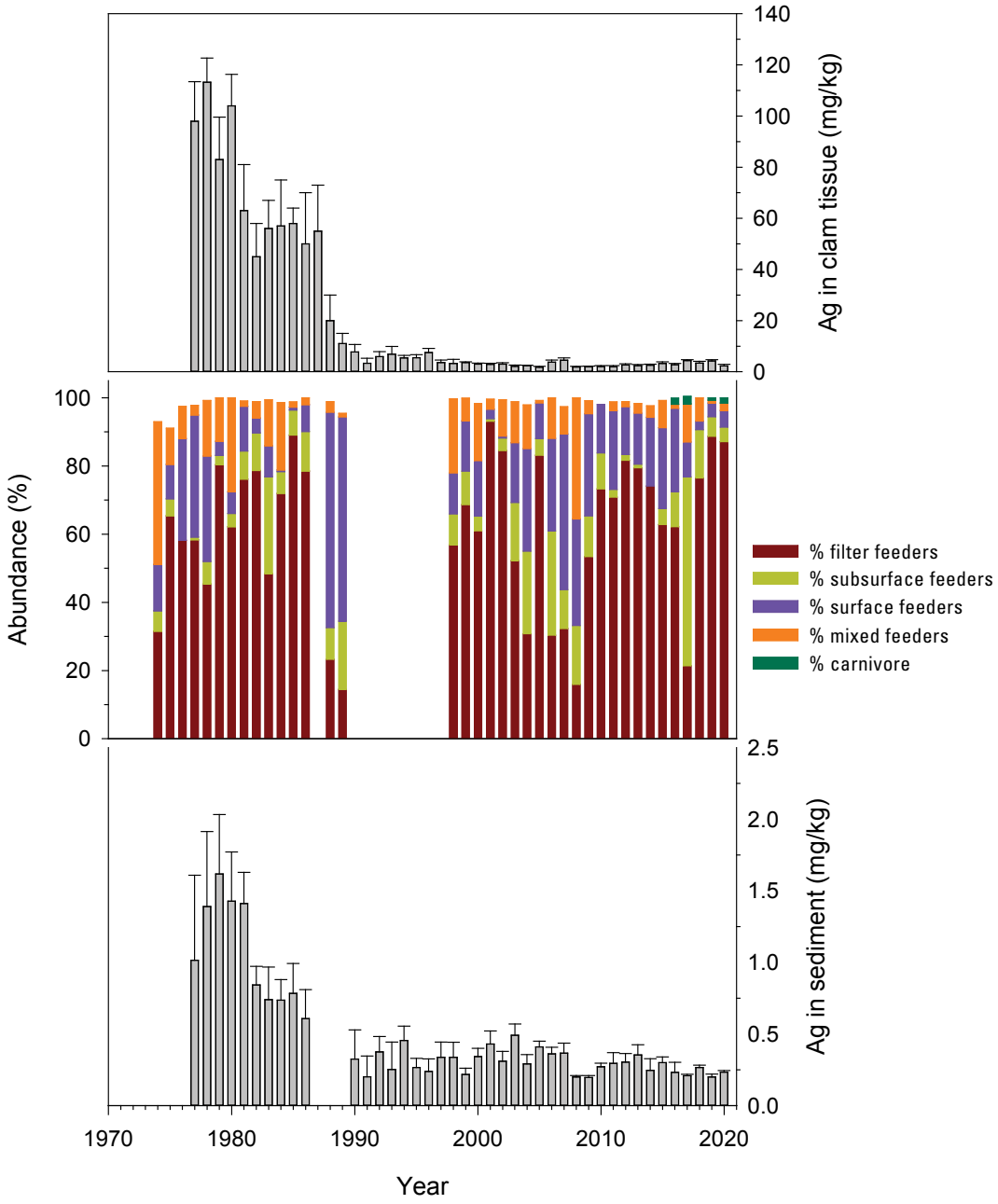

Figure 25. Graphs showing feeding-mode annual abundances for top-10-ranked species (middle), as well as silver (Ag) concentrations in clam *Limecola petalum* (top) and in sediment (bottom), at Palo Alto site, California, 1974–2020. Concentrations are grand mean ±standard error, in milligrams per kilogram (mg/kg); data were not collected in sediment from 1987 to 1989. Abundance data (in percent [%]) for each year are from August of that year (samples were not collected in 1987 nor from 1991 to 1997). Feeding modes: carnivore, preys on other infaunal invertebrates; filter, filters food particles from water column; mixed, capable of filter feeding and surface-deposit feeding; subsurface deposit, ingests subsurface sediment and removes food from sediment in gut; surface deposit, ingests food particles on surface sediment.

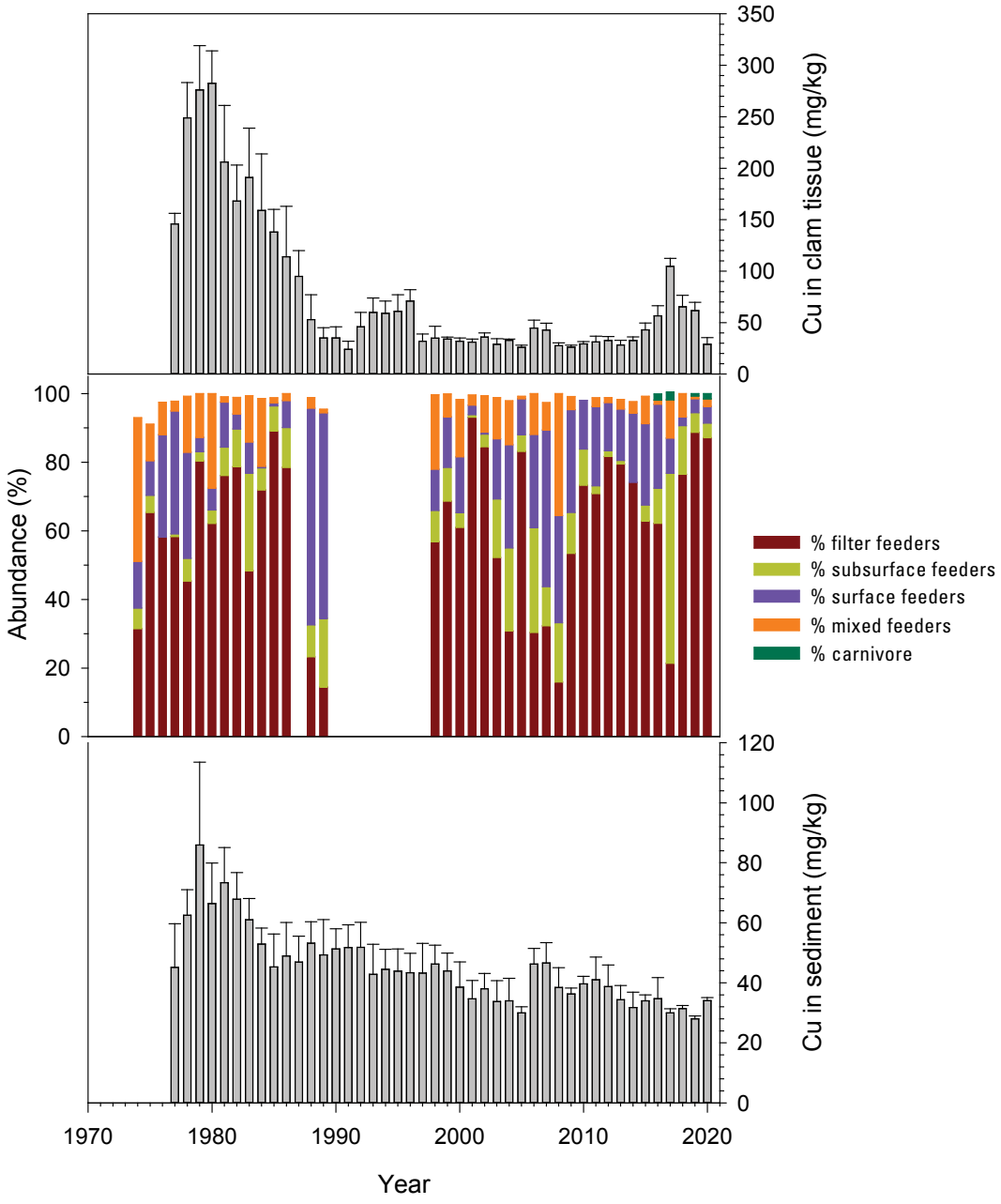

Figure 26. Graphs showing feeding-mode annual abundances for top-10-ranked species (middle), as well as copper (Cu) concentrations in clam *Limecola petalum* and in sediment, at Palo Alto site, California, 1974–2020. Concentrations are grand mean ±standard error, in milligrams per kilogram (mg/kg). Abundance data (in percent [%]) for each year are from August of that year (samples were not collected in 1987 nor from 1991 to 1997). Feeding modes: carnivore, preys on other infaunal invertebrates; filter, filters food particles from water column; mixed, capable of filter feeding and surface-deposit feeding; subsurface deposit, ingests subsurface sediment and removes food from sediment in gut; surface deposit, ingests food particles on surface sediment.

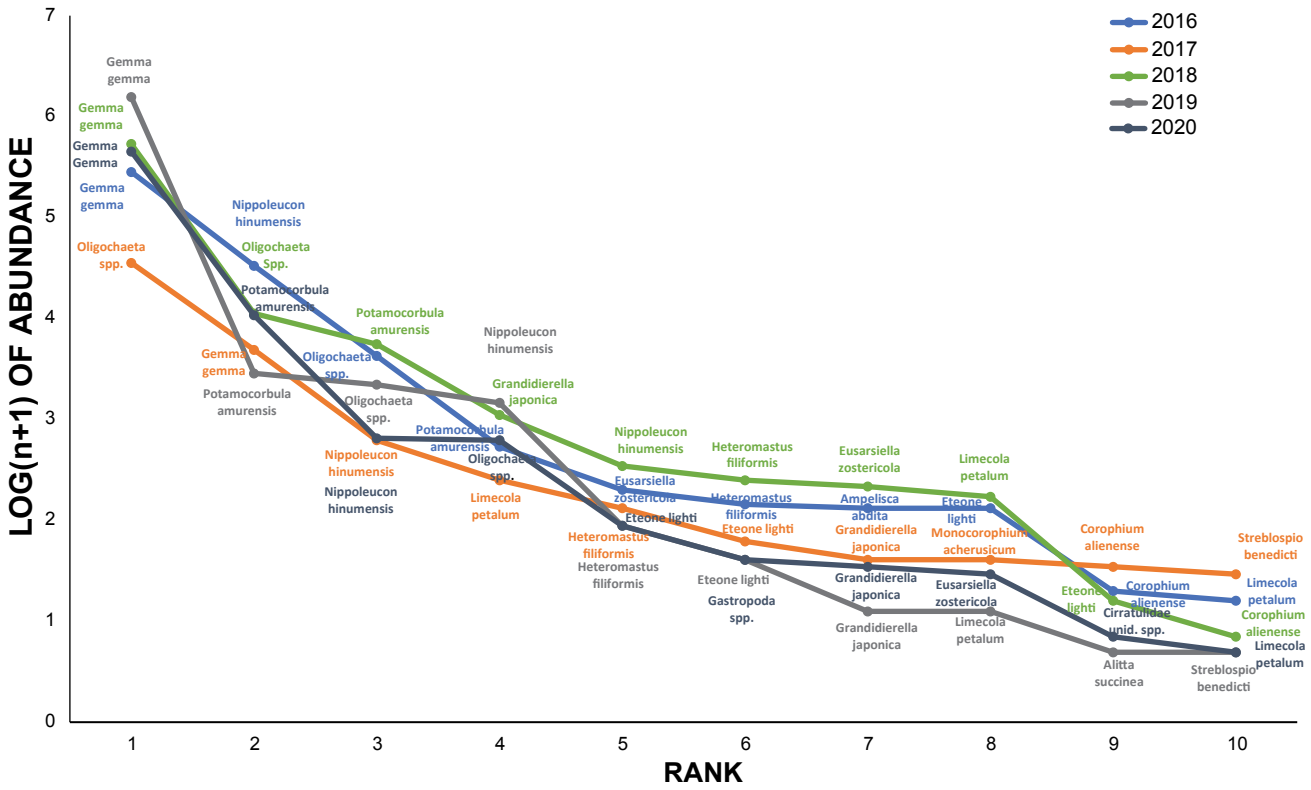

Figure 27. Graph showing species rank-abundance data for benthic community at Palo Alto site, California, 2016–2020.

benthic community with species dominance, as revealed by abundance, not showing large differences among the top 10 species. An examination of similar plots for August of three hydrologically dry years during this study (1977, 1989, and 2002) shows that the shape of the curve has changed greatly and that the 2020 curve is most similar to that seen in 2002 (fig. 28). Figure 28 depicts a community that was, with the rest of the species having similar abundances, heavily dominated by three species in 1977 and 1989 versus a community with one dominant species in 2002 and 2020. *G. gemma* is the most dominant species in all years except 1989. The 2020 curve shows a downward slope, which displays a homogenized decrease in species abundance (fig. 27). The 1977 community plot is the most extreme, with three species dominating the community and the remainder having similar but relatively low abundances.

It is informative to examine the rank-abundance graphs within the context of the life-history characteristics of each species. If shifts in plot shape coincide with a shift in community structure and function, that might be indicative of a healthier environment. Two critical life history characteristics are shown—feeding mode (fig. 29) and reproductive mode (fig. 30). The 1977 community was dominated by filter feeders (species that consume particles in the water column) and mixed feeders (species that have the option of either filter feeding or feeding on the sediment surface), as well as two species that feed on food particles on the sediment surface (fig. 29). In 1989, the species composition had shifted such that filter-feeding, subsurface-deposit-feeding, and surface-deposit-feeding species (that is, those that ingest sediment and strip the food off the sediment in their gut) dominated the community. In 2002, a shift was observed towards species that were mixed and subsurface-deposit feeders. The most recent data (2020) show the community to be similar to that of 2002, with the composition having shifted to that of filter-feeding species, subsurface-deposit-feeding species, and mixed-feeding species. During the period of this study, a shift has occurred from a community dominated by species that feed either in the water column or on recently settled food particles on the sediment surface to a mixed community of species that feed directly on the subsurface sediment, those that are capable of feeding in the water column, and those that feed on the sediment surface. The species that returned following the defaunation event in January and February 2008 have maintained this pattern. Thus, any sediment-borne pollutant is unlikely to have caused the collapse of the community in early 2008.

An examination of these rank-abundance plots using reproductive mode as the descriptor for each point is equally informative (fig. 30). The dominant species in 1977 were

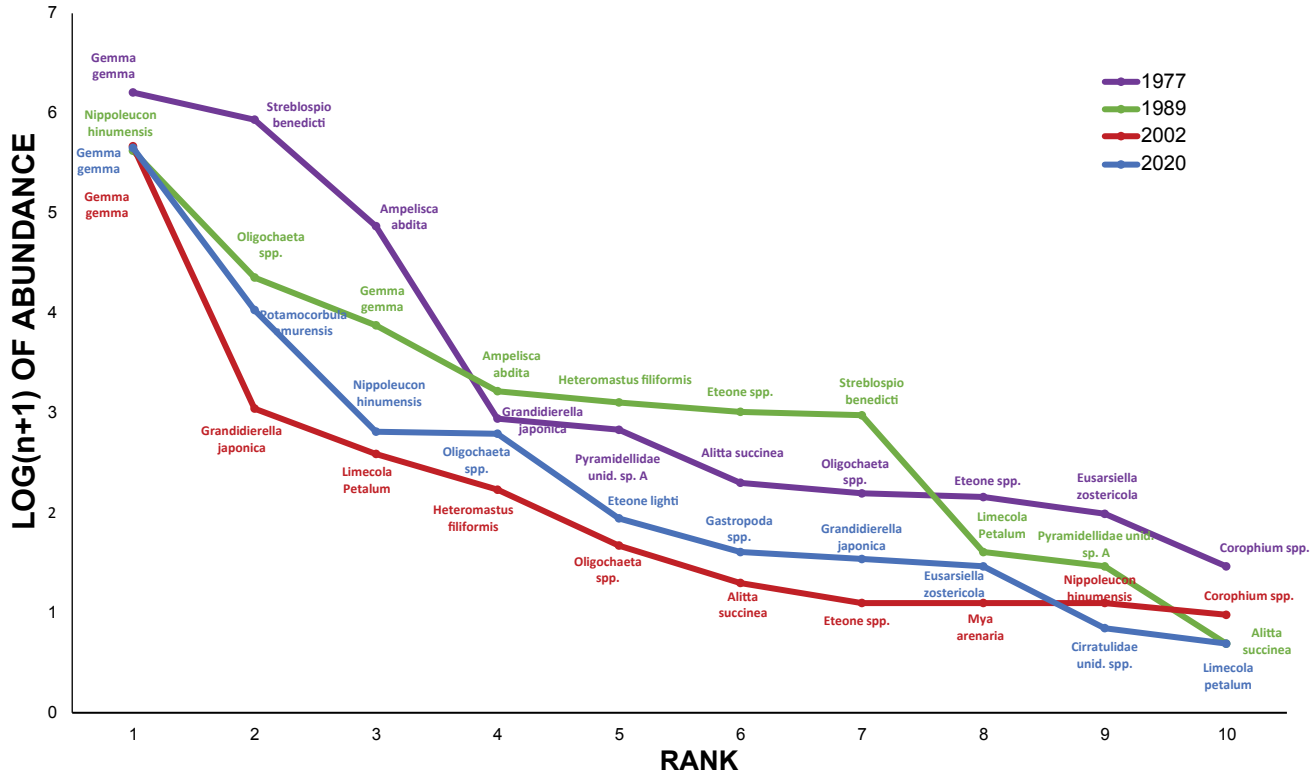

Figure 28. Graph showing species rank-abundance data for benthic community at Palo Alto site, California, 2016–2020.

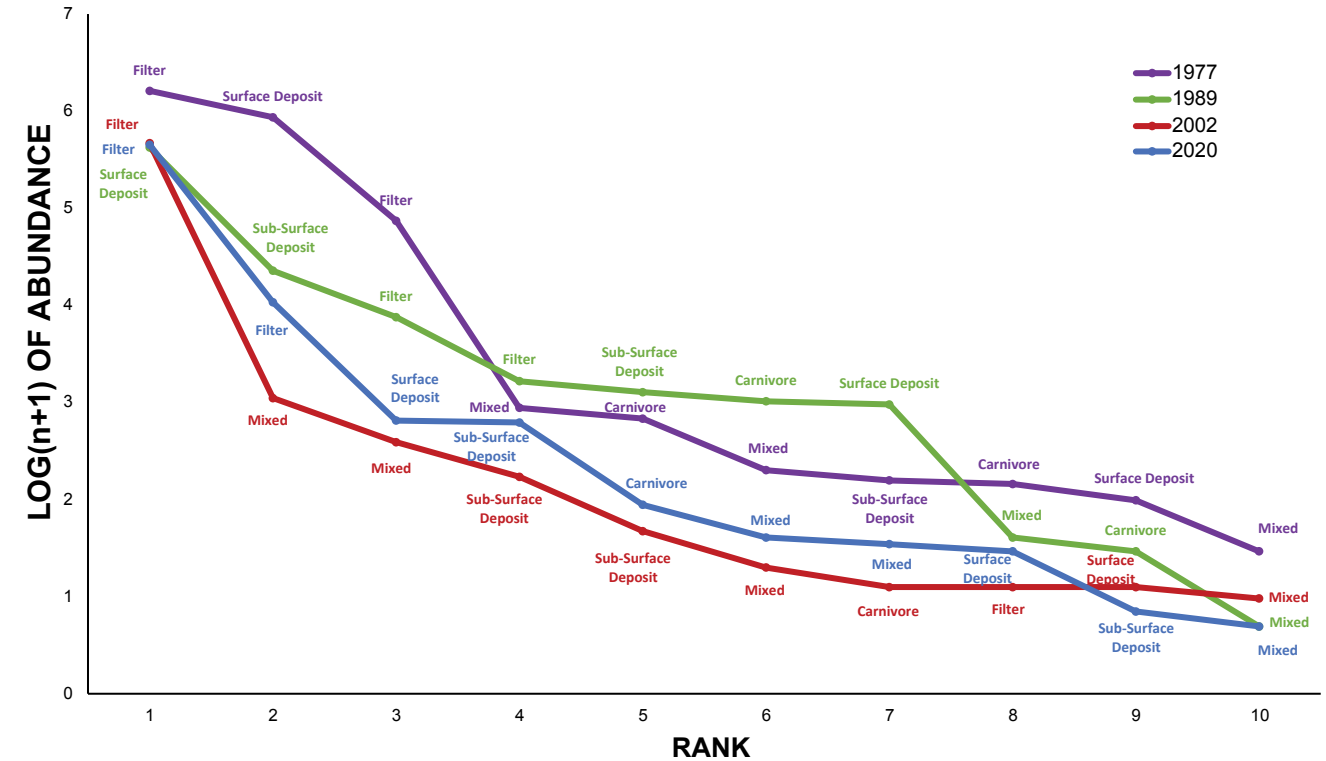

Figure 29. Graph showing species rank-abundance data identified by feeding modes of same benthic-community species shown in figure 28, at Palo Alto site, California, 1977, 1989, 2002, and 2020. Feeding modes: carnivore, predator on other fauna; filter, filters food particles from water column; mixed, capable of filter feeding and surface-deposit feeding; subsurface deposit, ingests subsurface sediment and removes food from sediment in gut; surface deposit, ingests food particles on surface sediment.

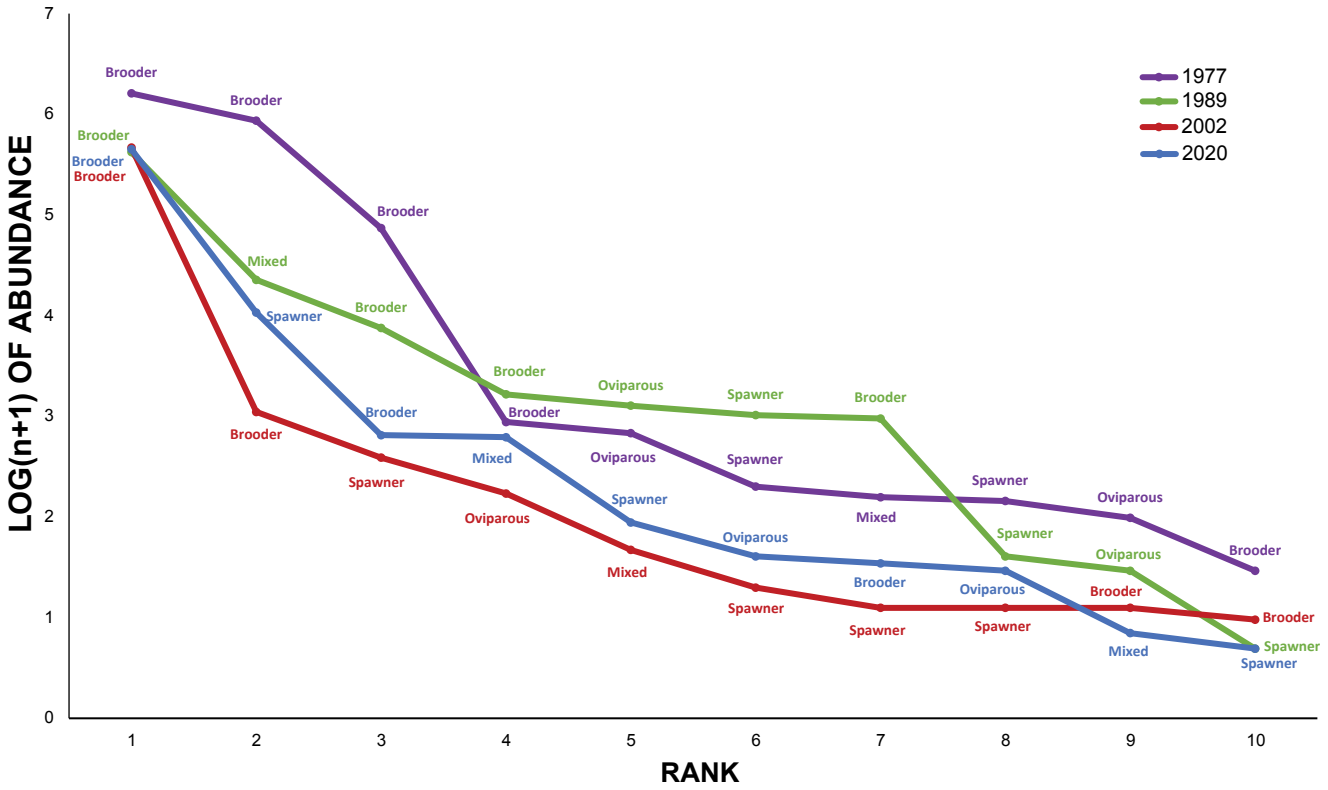

Figure 30. Graph showing species rank-abundance data identified by reproductive modes of same benthic-community species shown in figure 28, at Palo Alto site, California, 1977, 1989, 2002, and 2020. Reproductive modes: brooder, broods young and release juveniles as fully functional "miniature adults;" mixed, capable of ovipary and brooding; oviparous, lays eggs in or on sediment; spawner, releases gametes into water column and juveniles settle out of plankton onto sediment surface after growth in plankton.

species that brood their young and release fully functional juveniles into the environment. In 1989, several brooders were still present, but two species that lay their eggs in the sediment were also present. Although brooding species remain the most abundant species for all years, species that spawn their gametes into the water column—in combination with those that lay eggs in the sediment (oviparous)—have an equal presence. Some of the metal contaminants found in the sediment in the 1970s at this location possibly limited the success of species that consumed the sediment for food, laid eggs in the sediment, or depended on water-borne larvae to repopulate the community. Interestingly, at present (2020) the reproductive mode of most species is brooding, with some mixed egg-laying (oviparous) and spawning species (fig. 30).

Summary

Long-Term Observations

Since 1974, U.S. Geological Survey (USGS) personnel have monitored and conducted basic research on the benthic sediments and biological community near the discharge of the Palo Alto Regional Water Quality Control Plant (PARWQCP). The time series presented here updates and extends previous findings (for example, Luoma and others, 1991, 1995a, 1996; Hornberger and others, 2000; Thompson and others, 2002; Shouse and others, 2003, 2004; Moon and others, 2005; Cain and others, 2006; Dyke and others, 2012, 2014) with additional data from January 2020 through December 2020 to create a record spanning more than 40 years. This long-term dataset includes sediment chemistry and tissue concentrations of metals (1977–2020 for copper and silver; 1994–2020 for other metals), condition index (CI) (1988–2020), and reproductive activity in *Limecola petalum* and population dynamics of benthic invertebrate species (1974–2020). The time series encompasses the period when high concentrations of copper and silver were present in sediment and *L. petalum* (1970s and early 1980s) and the subsequent period when those concentrations declined. The sustained record of biogeochemical data at this site provides a rare opportunity to examine the biological response to metal contamination within this ecosystem over multiple time scales.

Studies during the 1970s showed that sediments and *L. petalum* at the Palo Alto site contained highly elevated concentrations of metals, especially silver and copper, as a result of metal-containing effluent being discharged from the PARWQCP to south San Francisco Bay. In the early 1980s, the point-source metal loading from the nearby PARWQCP was substantially reduced as a result of advanced treatment of influent and source mitigation. Coincident with decreases in

metal loadings, concentrations of metals in the sediment and in the clam *L. petalum* (serving as a biomonitor of metal exposures) also decreased, as previously described by Hornberger and others (2000). Interannual trends in clams and sediments were highly correlated with copper loadings from PARWQCP (concurrent loading data for silver were not available). Metal concentrations in sediments and clams responded relatively quickly to changes in metal loading; the reduction in metal loadings by the PARWQCP resulted in a decrease in metal concentrations in the sediment and *L. petalum* within a year (Hornberger and others, 2000).

Biological responses to metal inputs to south San Francisco Bay were assessed at different levels of organization. These responses are interpreted within the appropriate temporal context. Because metal exposures were already high when the study began, interpretations are based on observed changes in biological attributes as metal inputs decreased. In general, discernible responses at the organism level (that is, reproductive activity, a manifestation of a cellular or physiological change) to metal exposure may occur within a relatively short time (for example, at intra-annual and inter-annual time scales, as previously exposed individuals recover and successive cohorts become established), whereas population- and community-level responses take longer to develop. Stable changes in the benthic community may take a relatively long period of time to be expressed because of the normally high degree of intra-annual variability of benthic community dynamics, which reflects the cumulative response to natural and anthropogenic disturbances. It is therefore critical that sampling frequency and duration be conducted at temporal scales appropriate to characterize the different biological responses.

During the first 10 years of this study, when the metal concentrations were initially high and decreasing, the benthic community was largely dominated by nonindigenous, opportunistic species. This dominance was initially attributed to their ability to survive the many physical disturbances on the mudflat (Nichols and Thompson, 1985a, 1985b), for example, sediment erosion and deposition, as well as aerial exposure at extreme low tides. The possible effects of metal exposure as a disturbance factor were not considered in the analyses by Nichols and Thompson (1985a, 1985b) because the decrease in metal concentrations in *L. petalum* and sediment had just begun.

However, biological responses throughout the period of decreasing metal exposure emerged. Reproductive activity improved within a year or two of reduced metal exposure (Hornberger and others, 2000), and responses at the population and community levels were observed afterward. Identification of these responses was possible because the frequency of sampling allowed long-term trends related to metal contamination to be identified within the context of repeating seasonal cycles and unrelated intra-annual variation.

The ecology of the Palo Alto mudflats is part of the larger south San Francisco Bay, which has been undergoing some changes in recent years. From 1999 to 2005, USGS scientists noticed an increase in phytoplankton biomass in the southern part of the bay. Sampling in the deeper water of the southern part of the bay showed that bivalves were mostly absent from the system during this increase in primary production. Cloern and others (2007) indicated that the cause of the decrease in bivalves was an increase in fish predators resulting from increased offshore upwelling activity. The higher reproductive success of demersal fish, crabs, and shrimp during this period resulted in a higher number of juveniles moving into south San Francisco Bay to grow. Since 2005, scientists have seen the large bivalve populations fluctuate more than in previous decades, and these fluctuations have been reflected in changes in phytoplankton biomass in the system (primarily through an increase in phytoplankton biomass in late summer and fall). The value of these findings in the greater south San Francisco Bay to this study is twofold. First, it reinforces the importance of the benthic community's impact on ecosystem function and solute cycling. Second, it shows that the high intertidal community at the Palo Alto site has not been demonstrably affected by these greater south San Francisco Bay influences during these years. These findings reinforce our confidence that the changes observed in the benthic community are in large part owing to local factors.

2020 Observations

Throughout 2020, copper and silver concentrations in sediments remained representative of the concentrations observed since 1990, after the significant reductions in concentrations during the 1980s that coincided with reductions in the discharge of these elements from PARWQCP. Since 1994, annual mean copper and silver concentrations have fluctuated modestly but have trended downward. Zinc and iron also have drifted downward. Sedimentary concentrations of other elements have varied from year to year but shown no sustained temporal trend.

Most metal concentrations in *L. petalum* during 2020 are comparable to the concentrations observed since the 1990s. Mercury concentrations measured in 2020 were slightly lower than in recent years and remained high relative to the long-term record. Mercury concentrations were highest in 3 of the past 5 years. The relatively high concentrations in 2017 and 2020 affect the upward trend in mercury since 1994. Downward trends in inter-annual concentrations of silver and zinc in *L. petalum* appear to be related to the CI, a metric of the general physiological condition of the clam. In contrast, the variation of other metals appeared to be independent of the CI and sediment metal concentrations.

The long-term data series suggest that contemporary metal concentrations in sediments and tissue of *L. petalum* likely reflect a combination of factors. These may include inputs from the PARWQCP and other south San Francisco Bay point sources, inputs from local streams and stormwater conveyances, cycling of contaminants stored within bay sediments, and regionally scaled physical and biogeochemical processes controlling the distribution and bioavailability of metals.

The long-term dataset that we augment with this report demonstrates various adverse effects of contaminants on benthic organisms. Decreasing particulate concentrations of trace metals in the local environment have benefited resident populations of invertebrates, as shown by increased reproductive activity in *L. petalum* that has been sustained through the present (2020). In early 2008, the benthic community decreased, with few animals present in February. This decrease was likely the result of a natural stressor, such as a sedimentation or freshwater inundation event, and the composition of the benthic community supports that supposition. Mobile animals such as *L. petalum* that were capable of burrowing down to avoid the stressor probably did so, but many other species either relocated or did not survive at the study site. This natural disturbance gives scientists the opportunity to observe mudflat community recovery from a natural stressor and to compare this recovery to that observed during the long-term decrease of metals in sediment and *L. petalum*. Shifts in species abundance at the study site have been interpreted to be a response to decreasing sediment contaminants within 2 years of improved wastewater treatment at PARWQCP. These community changes have included a shift from species that live on the surface, filter food out of the water column, or consume particles on the sediment surface and brood their young to a community dominated by species that live on and below the surface, consume the sediment directly to harvest food particles, and spawn and lay eggs in the sediment. Hence, the benthic community now has a greater dependence on sediment for food and reproduction relative to the late 1970s, consistent with management practices that have improved sediment quality. The data from 2008 to 2020 reveal a community that had a short-term physical stressor but not a community that was subject to trace-metal contamination. At present (2020), the species abundance data continues to show signs of a community that has recovered and stabilized, and the constancy of functional groups reflects the stability of the ecosystem. Thus, the data from the recent record (that is, within the three decades prior to 2020) reflect the improved ecological condition of the Palo Alto site, which is indicative of an integrated regional ecological baseline. This "natural experiment" has given USGS scientists an opportunity to test various hypotheses on the benthic community's response to different stressors. Future data will continue to refine the understanding of the response of this benthic community to natural and anthropogenic stressors.

Value of Long-Term Monitoring

This study highlights the importance of long-term ecosystem monitoring. Although monitoring studies cannot always unambiguously determine the causes of variation in metal concentrations or benthic community structure, time-series data may reveal ecological responses that are distinctively associated with human activities. Changes and trends in community structure that may be related to anthropogenic stressors, as was seen in this study for multiple trace metals, can be established only with a concerted and committed sampling effort of sufficient duration and frequency and data interpretation. The strength and uniqueness of this study is the integrated analysis of metal exposure and biological response at intra-annual and inter-annual time scales over multiple decades.

Human activities have and will continue to change south San Francisco Bay and its watershed. Factors that may influence metals in the near and long term include climate variation, nonpoint-source runoff and efforts to mitigate it, reconnection of reclaimed intertidal areas to the bay, cycling of legacy contamination within the bay, new and redevelopment of the Bay Area landscape, and sea-level rise. Among emerging contaminants of concern are metal-based nanomaterials, many of which include metal-based products in forms that environmental scientists and regulators have little or no experience with. Quantitative descriptions of the bioavailability of trace metals from such sources have only recently been reported (for example, Croteau and others, 2011, 2014). The long-term, detailed, integrated ecological baseline that has been established at this sampling site will be immensely valuable in assessing the response of the environment and informing management and regulatory agencies as human activities within the watershed continue.

References Cited

Ahn, I.-Y., Kang, Y.-C., and Choi, J.-W., 1995, The influence of industrial effluents on intertidal benthic communities in Panweol, Kyeonggi Bay (Yellow Sea) on the west coast of Korea: Marine Pollution Bulletin, v. 30, no. 3, p. 200–206, https://doi.org/10.1016/0025-326X(94)00125-S.

Alpine, A.E., and Cloern, J.E., 1992, Trophic interactions and direct physical effects control phytoplankton biomass and production in an estuary: Limnology and Oceanography, v. 37, no. 5, p. 946–955, https://doi.org/10.4319/lo.1992.37.5.0946.

Cain, D.J., Croteau, M., Parchaso, F., Stewart, R., Zierdt Smith, E.L., Thompson, J.K., Kieu, L., Turner, M., and Baesman, S.M., 2022, Data for monitoring trace metal and benthic community near the Palo Alto Regional Water Quality Control Plant in South San Francisco Bay, California (ver 2.0, November 2022): U.S. Geological Survey data release, https://doi.org/10.5066/P9IBQ23S

Cain, D.J., Croteau, M.-N., Thompson, J.K., Parchaso, F., Stewart, R., Shrader, K.H., Zierdt Smith, E.L., and Luoma, S.N., 2021, Near-field receiving-water monitoring of trace metals and a benthic community near the Palo Alto Regional Water Quality Control Plant in south San Francisco Bay, California—2019: U.S. Geological Survey Open-File Report 2021–1079, 59 p., https://doi.org/10.3133/ofr20211079.

Cain, D.J., and Luoma, S.N., 1990, Influence of seasonal growth, age, and environmental exposure on Cu and Ag in a bivalve indicator, *Macoma balthica*, in San Francisco Bay: Marine Ecology Progress Series, v. 60, p. 45–55.

Cain, D.J., Parchaso, F., Thompson, J.K., Luoma, S.N., Lorenzi, A.H., Moon, E., Shouse, M.K., Hornberger, M.I., and Dyke, J.L., 2006, Near-field receiving water monitoring of trace metals and a benthic community near the Palo Alto Regional Water Quality Control Plant in south San Francisco Bay, California—2005: U.S. Geological Survey Open-File Report 2006–1152, 120 p., https://doi.org/10.3133/ofr20061152.

Childress, C.J.O., Foreman, W.T., Connor, B.F., and Maloney, T.J., 1999, New reporting procedures based on long-term method detection levels and some considerations for interpretations of water-quality data provided by the U.S. Geological Survey National Water Quality Laboratory: U.S. Geological Survey Open-File Report 99–193, 19 p., https://doi.org/10.3133/ofr99193.

Cloern, J.E., Jassby, A.D., Thompson, J.K., and Hieb, K.A., 2007, A cold phase of the East Pacific triggers new phytoplankton blooms in San Francisco Bay: Proceedings of the National Academy of Science, v. 104, no. 47, p. 18,561–18,565, https://doi.org/10.1073/pnas.0706151104.

Cohen, A.N., and Carlton, J.T., 1995, Biological study—Nonindigenous aquatic species in a United States estuary—A case study of the biological invasions of the San Francisco Bay and Delta: Washington, D.C., Report for the U.S. Fish and Wildlife Service and the National Sea Grant College Program, Connecticut Sea Grant, accessed July 12, 2019, at https://www.scribd.com/document/106882160/Cohen-Carlton-1995-San-Francisco-Bay-Invasion-Report#.

Croteau, M.-N., Misra, S.K., Luoma, S.N., and Valsami-Jones, E., 2011, Silver bioaccumulation dynamics in a freshwater invertebrate after aqueous and dietary exposures to nanosized and ionic Ag: Environmental Science & Technology, v. 45, no. 15, p. 6660–6607, https://doi.org/10.1021/es200880c.

Croteau, M.-N., Misra, S.K., Luoma, S.N., and Valsami-Jones, E., 2014, Bioaccumulation and toxicity of CuO nanoparticles by a freshwater invertebrate after waterborne and dietborne exposures: Environmental Science & Technology, v. 48, no. 18, p. 10,929–10,937, https://doi.org/10.1021/es5018703.

David, C.P.C., Luoma, S.N., Brown, C.L., Cain, D.J., Hornberger, M.I., and Lavigne, I.R., 2002, Near field receiving water monitoring of trace metals in clams (*Macoma balthica*) and sediments near the Palo Alto Water Quality Control Plant in south San Francisco Bay, California—1999–2001: U.S. Geological Survey Open-File Report 2002–453, 44 p., https://doi.org/10.3133/ofr02453.

Dell Inc., 2016, Statistica, version 13.2: Dell, Inc. software release.

Dyke, J.L., Cain, D.J., Thompson, J.K., Kleckner, A.E., Parchaso, F., Hornberger, M.I., and Luoma, S.N., 2014, Near-field receiving water monitoring of trace metals and a benthic community near the Palo Alto Regional Water Quality Control Plant in south San Francisco Bay, California—2013: U.S. Geological Survey Open-File Report 2014–1174, 81 p., https://doi.org/10.3133/ofr20141174.

Dyke, J.L., Thompson, J.K., Cain, D.J., Kleckner, A.E., Parchaso, F., Luoma, S.N., and Hornberger, M.I., 2012, Near-field receiving water monitoring of trace metals and a benthic community near the Palo Alto Regional Water Quality Control Plant in south San Francisco Bay, California—2011: U.S. Geological Survey Open-File Report 2012–1165, 108 p., https://doi.org/10.3133/ofr20121165.

Dyke, J.L., Parchaso, F., Thompson, J.K., Cain, D.J., Luoma, S.N., and Hornberger, M.I., 2010, Near-field receiving water monitoring of trace metals and a benthic community near the Palo Alto Regional Water Quality Control Plant in South San Francisco Bay, California—2009: U.S. Geological Survey Open-File Report 2010-1188, 142 p., https://pubs.usgs.gov/of/2010/1188/.

Elrick, K.A., and Horowitz, A.J., 1985, Analysis of rocks and sediments for arsenic, antimony, and selenium, by wet digestion and hydride atomic absorption: U.S. Geological Survey Open-File Report 85–497, 14 p., https://doi.org/10.3133/ofr85497.

Förstner, U., and Wittmann, G.T.W., 1981, Metal pollution in the aquatic environment: Berlin, Zeitschrift für allgemeine Mikrobiologie, v. 21, no. 7, p. 564, https://doi.org/10.1002/jobm.19810210712.

Glaser, J.A., Foerst, D.L., McKee, G.D., Quave, S.A., and Budde, W.L., 1981, Trace analyses for wastewaters: Environmental Science & Technology, v. 15, no. 12, p. 1426–1435, https://doi.org/10.1021/es00094a002.

Hook, S.E., and Fisher, N.S., 2001, Sublethal effects of silver in zooplankton—Importance of exposure pathways and implications for toxicity testing: Environmental Toxicology and Chemistry, v. 20, no. 3, p. 568–574, https://doi.org/10.1002/etc.5620200316.

Hook, S.E., and Fisher, N.S., 2002, Relating the reproductive toxicity of five ingested metals in calanoid copepods with sulfur affinity: Marine Environmental Research, v. 53, no. 2, p. 161–174, https://doi.org/10.1016/S0141-1136(01)00118-0.

Hornberger, M.I., Luoma, S.N., Cain, D.J., Parchaso, F., Brown, C.L., Bouse, R.M., Wellise, C., and Thompson, J.K., 2000, Linkage of bioaccumulation and biological effects to changes in pollutant loads in south San Francisco Bay: Environmental Science & Technology, v. 34, no. 12, p. 2401–2409, https://doi.org/10.1021/es991185g.

Hornberger, M.I., Luoma, S.N., van Geen, A., Fuller, C.., and Anima, R., 1999, Historical trends of metals in the sediments of San Francisco Bay, California: Marine Chemistry, v. 64, nos. 1–2, p. 39–55, https://doi.org/10.1016/S0304-4203(98)80083-2.

Kennish, M.J., 1998, Pollution impacts on marine biotic communities: Boca Raton, Fla., CRC Press, 336 p., https://doi.org/10.1201/9781003069003.

Kleckner, A.E., Kakouros, E., and Stewart, A.R., 2017, A practical method for the determination of total selenium in environmental samples using isotope dilution-hydride generation-inductively coupled plasma-mass spectrometry: Limnology and Oceanography Methods, v. 15, no. 4, p. 363–371, https://doi.org/10.1002/lom3.10164.

Long, E.R., MacDonald, D.D., Smith, S.L., and Calder, F.D., 1995, Incidence of adverse biological effects within ranges of chemical concentrations in marine and estuarine sediments: Environmental Management, v. 19, no. 1, p. 81–97, https://doi.org/10.1007/BF02472006.

Luoma, S.N., Cain, D.J., Brown, C., and Axtmann, E.V., 1991, Trace metals in clams (*Macoma balthica*) and sediments at the Palo Alto mudflat in south San Francisco Bay—April, 1990–April, 1991: U.S. Geological Survey Open-File Report 91–460, 47 p., https://doi.org/10.3133/ofr91460.

Luoma, S.N., Cain, D.J., Brown, C.L., Hornberger, M.I., and Bouse Schaenemann, R.M., 1995a, Near field receiving water monitoring of trace metals in clams (*Macoma balthica*) and sediments near the Palo Alto and San Jose/Sunnyvale Water Quality Control Plants in south San Francisco Bay—June 1993 through October 1994: U.S. Geological Survey Open-File Report 95–299, 83 p., https://doi.org/10.3133/ofr95299.

Luoma, S.N., Cain, D.J., Brown, C., Hornberger, M., and Bouse, R., 1996, Near field receiving water monitoring of trace metals in clams (*Macoma balthica*) and sediments near the Palo Alto and San Jose/Sunnyvale Water Quality Control Plants in south San Francisco Bay—December 1994–December 1995: U.S. Geological Survey Open-File Report 96–203, 90 p., https://doi.org/10.3133/ofr96203.

Luoma, S.N., Cain, D., and Johansson, C., 1985, Temporal fluctuations of silver, copper and zinc in the bivalve *Macoma balthica* at five stations in South San Francisco Bay: Hydrobiologia, v. 129, p. 109–120, https://doi.org/10.1007/BF00048690.

Luoma, S.N., and Cloern, J.E., 1982, The impact of waste-water discharge on biological communities in San Francisco Bay, *in* Kockelman, W.J., ed., San Francisco Bay—The urbanized estuary: San Francisco, Calif., American Association for the Advancement of Science, p. 137–160, https://pubs.er.usgs.gov/publication/70156948.

Luoma, S.N., Ho, Y.B., and. Bryan, G.W., 1995b, Fate, bioavailability and toxicity of silver in estuarine environments: Marine Pollution Bulletin, v. 31, nos. 1–3, p. 44–54, https://doi.org/10.1016/0025-326X(95)00081-W.

Moon, E., Shouse, M.K., Parchaso, F., Thompson, J.K., Luoma, S.N., Cain, D.J., and Hornberger, M.I., 2005, Near-field receiving water monitoring of trace metals and a benthic community near the Palo Alto Regional Water Quality Control Plant in South San Francisco Bay, California—2004: U.S. Geological Survey Open-File Report 2005–1279, 72 p. plus appendixes, https://doi.org/10.3133/ofr20051279.

Morrisey, D.J., Underwood, A.J., and Howitt, L., 1996, Effects of copper on the faunas of marine soft-sediments—An experimental field study: Marine Biology, v. 125, p. 199–213, https://doi.org/10.1007/BF00350774.

Newman, M.C., 1998, Fundamentals of ecotoxicology: Chelsea, Mich., Sleeping Bear Press, 402 p.

Nichols, F.H., and Thompson, J.K., 1985a, Persistence of an introduced mudflat community in South San Francisco Bay, California: Marine Ecology - Progress Series, v. 24, p. 83–97, https://doi.org/10.3354/meps024083.

Nichols, F.H., and Thompson, J.K., 1985b, Time scales of change in the San Francisco Bay benthos: Hydrobiologia, v. 129, p. 121–138, https://doi.org/10.1007/BF00048691.

Parchaso, F., 1993, Seasonal reproduction of *Potamocorbula amurensis* in San Francisco Bay, California: San Francisco, Calif., San Francisco State University, M.S. thesis, 43 p.

Phillips, D.J.H., and Rainbow, P.S., 1993, Biomonitoring of trace aquatic contaminants: Barking, England, Elsevier Science Publishers, LTD, 371 p.

Rasmussen, E., 1956, The reproduction and larval development of some polychaetes from the Isefjord, with some faunistic notes: Biologiske Meddelelser, det Kongelige Danske Videnskabernes Selskab, v. 23, no. 1, p. 1–84.

Rygg, B., 1985, Effect of sediment copper on benthic fauna: Marine Ecology - Progress Series, v. 25, p. 83–89, https://doi.org/10.3354/meps025083.

San Francisco Estuary Institute, 1997, 1996 annual report—San Francisco Estuary Regional Monitoring Program for trace substances: Richmond, Calif., San Francisco Estuary Institute, 299 p. plus appendixes.

San Francisco Estuary Institute, 2016, 2015 Annual Monitoring Report—San Francisco Estuary Regional Monitoring Program for water quality in the San Francisco Bay: Richmond, Calif., San Francisco Estuary Institute, contribution no. 775, 19 p. plus appendixes.

Shouse, M.K., 2002, The effects of decreasing trace metal concentrations on benthic community structure: San Francisco, Calif., San Francisco State University, M.S. thesis, 177 p.

Shouse, M.K., Parchaso, F., and Thompson, J.K., 2003, Near-field receiving water monitoring of benthic community near the Palo Alto Water Quality Control Plant in South San Francisco Bay—February 1974 through December 2002: U.S. Geological Survey Open-File Report 03–224, 39 p., https://doi.org/10.3133/ofr03224.

Shouse, M.K., Parchaso, F., and Thompson, J.K., 2004, Near-field receiving water monitoring of a benthic community near the Palo Alto Water Quality Control Plant in South San Francisco Bay—February 1974 through December 2003: U.S. Geological Survey Open-File Report 2004–1210, 37 p. plus appendixes, https://doi.org/10.3133/ofr20041210.

Simon, T.P., ed., 2002, Biological response signatures—Indicator patterns using aquatic communities: Boca Raton, Fla., CRC Press, 600 p., https://doi.org/10.1201/9781420041453.

Suter, G.W., II, 2001, Applicability of indicator monitoring to ecological risk assessment: Ecological Indicators, v. 1, no. 2, p. 101–112, https://doi.org/10.1016/S1470-160X(01)00011-5.

Thompson, J.K., and Parchaso, F., 2012, Benthic invertebrate community assessment as a phytoplankton consumer and fish and bird prey source before and after the start of the restoration: South Bay Salt Pond Restoration Project Cooperative Agreement 2009–0211, 26 p. plus appendixes.

Thompson, J.K., Parchaso, F., and Shouse, M.K., 2002, Near field receiving water monitoring of benthic community near the Palo Alto Water Quality Control Plant in South San Francisco Bay—February 1974 through December 2000: U.S. Geological Survey Open-File Report 02–394, 33 p. plus appendixes, https://doi.org/10.3133/ofr02394.

Thomson, E.A., Luoma, S.N., Johansson, C.E., and Cain, D.J., 1984, Comparison of sediments and organisms in identifying sources of biologically available trace metal contamination: Water Research, v. 18, no. 6, p. 755–765, https://doi.org/10.1016/0043-1354(84)90172-6.

Thomson-Becker, E.A., and Luoma, S.N., 1985, Temporal fluctuations in grain size, organic materials and iron concentrations in intertidal surface sediment of San Francisco Bay: Hydrobiologia, v. 129, p. 91–107, https://doi.org/10.1007/BF00048689.

Topping, B.R., and Kuwabara, J.S., 2003, Dissolved nickel and benthic flux in south San Francisco Bay—A potential for natural sources to dominate: Bulletin of Environmental Contamination and Toxicology, v. 71, p. 46–51, https://doi.org/10.1007/s00128-003-0129-7.

U.S. Environmental Protection Agency, 2002, Method 1631, Revision E—Mercury in water by oxidation, purge and trap, and cold vapor atomic fluorescence spectrometry: Washington, D.C., U.S. Environmental Protection Agency EPA–821–R–02–019, 38 p.

U.S. Environmental Protection Agency, 1994, Method 200.7—Determination of metals and trace elements in water and wastes by inductively coupled plasma-atomic emission spectrometry, Revision 4.4: Cincinnati, Ohio, U.S. Environmental Protection Agency, accessed March 4, 2023, at https://www.epa.gov/esam/method-2007-determination-metals-and-trace-elements-water-and-wastes-inductively-coupled.

U.S. Environmental Protection Agency, 2004, Revised assessment of detection and quantitation approaches: Washington, D.C., U.S. Environmental Protection Agency EPA–821–B–04–005, 254 p.

U.S. Environmental Protection Agency, 1996, Method 3050B—Acid Digestion of Sediments, Sludges, and Soils, Revision 2: U.S. Environmental Protection Agency, 12p., accessed March 4, 2023, at https://www.epa.gov/esam/epa-method-3050b-acid-digestion-sediments-sludges-and-soils.

van Geen, A., and Luoma, S.N., 1999, The impact of human activities on sediments of San Francisco Bay, California—An overview: Marine Chemistry, v. 64, nos. 1–2, p. 1–6, https://doi.org/10.1016/S0304-4203(98)00080-2.

Wang, W.-X., and Fisher, N.S., 1999, Delineating metal accumulation pathways for marine invertebrates: Science of The Total Environment, v. 237–238, p. 459–472, https://doi.org/10.1016/S0048-9697(99)00158-8.

Weesner, F.M., 1960, General zoological microtechniques: Baltimore, Md., Williams & Wilkins, 230 p.

Whittaker, R.H., 1965, Dominance and diversity in land plant communities—Numerical relations of species express the importance of competition in community function and evolution: Science, v. 147, no. 3655, p. 250–260, https://doi.org/10.1126/science.147.3655.250.

World Register of Marine Species, 2020, WoRMS Taxon Match: World Register of Marine Species database, accessed December 29, 2020, at https://doi.org/10.14284/170.

Appendixes 1–9

Appendix 1. Certified Concentrations and Recovery Percentages of Inorganic Elements in National Institute of Science and Technology Standard Reference Materials 2709a and 2711a, Prepared in 2020

Table 1.1. Certified concentrations and recovery percentages of inorganic elements in National Institute of Science and Technology (NIST) standard reference materials 2709a (San Joaquin Soil) and 2711a (Montana II Soil), prepared in 2020.

[Standard reference materials (SRM) issued by National Institute of Science and Technology (NIST) (https://www.nist.gov). Abbreviations: CI, 95-percent confidence interval; mg/kg, milligram per kilogram; na, not applicable; nc, not certified; %, percent]

Reference material	Element	Sample size	Certified value (mg/kg)	Recovery mean ±CI (%)
2709a (San Joaquin Soil)	Aluminum	16	73,700	33±1
	Chromium	16	130	60±1
	Copper	16	33.9	78±1
	Iron	16	33,600	84±1
	Nickel	16	85	90±1
	Silver	na	nc	na
	Zinc	16	103	87±2
2711a (Montana II Soil)	Aluminum	16	67,200	31±1
	Chromium	16	52.3	45±2
	Copper	16	140	91±1
	Iron	16	28,200	78±2
	Nickel	16	21.7	86±2
	Silver	16	6	89±2
	Zinc	16	414	93±2

Appendix 2. Certified Concentrations and Recovery Percentages of Inorganic Elements in National Research Council Canada Certified Reference Material TORT-3 and National Institute of Science and Technology Standard Reference Material 1566b, Prepared in 2020

Table 2.1. Certified concentrations and recovery percentages of inorganic elements in National Research Council Canada (NRCC) certified reference material TORT-3 (lobster hepatopancreas) and National Institute of Science and Technology standard reference material 1566b (oyster tissue), prepared in 2020.

[Sources of reference materials (SRM): TORT-3 (lobster hepatopancreas), National Research Council Canada (https://nrc.canada.ca); 1566b (oyster tissue), National Institute of Science and Technology (https://www.nist.gov). Samples were not diluted prior to analysis. Abbreviations: CI, 95-percent confidence interval; mg/kg, milligram per kilogram; na, not applicable; nc, not certified; %, percent]

Reference material	Element	Sample size	Certified value (mg/kg)	Recovery mean ± int. (%)
TORT-3	Chromium	14	1.95	103±4
	Copper	14	497	91±2
	Nickel	14	5.3	84±1
	Silver	na	nc	na
	Zinc	14	136	93±2
1566b	Chromium	na	nc	na
	Copper	14	71.6	94±2
	Nickel	14	1.04	89±2
	Silver	14	0.666	93±1
	Zinc	14	1,424	104±2

Appendix 3. Mercury and Selenium Concentrations Determined in Sample Splits of Surface Sediments and Clam *Limecola petalum* Collected at Palo Alto Site, California, in 2020

Table 3.1. Mercury and selenium concentrations determined in sample splits of surface sediments and clam *Limecola petalum* collected at Palo Alto site, California, in 2020.

[One sediment sample and one clam tissue sample were split and analyzed for selenium and mercury; split results are shown here. Absolute deviation = difference between replicates ÷ 2. Abbreviations: CV, coefficient of variation [= (absolute deviation ÷ mean) × 100]; mg/kg, milligram per kilogram dry weight; na, not applicable; %, percent]

Sample type	Element	Sample	Measured concentration (mg/kg)	Mean	Absolute deviation	CV (%)
Sediment	Mercury	PA05132020	0.29	0.30	0.008	2.8
		PA05132020_LDUP	0.31	na	na	na
	Selenium	PA12112020	0.349	0.34	NR	2.66
		PA12112020_Dup	0.331	na	na	na
Tissue	Mercury	PA02172020_Lp3	0.64	0.63	0.014	2.3
		PA02172020_Lp3LDUP	0.62	na	na	na
		PA09192020_Lp3	0.25	0.25	0.0001	0.05
		PA09192020_Lp3LDUP	0.25	na	na	na
	Selenium	PA12112020_Lp3	2.85	2.68	NR	6.55
		PA12112020_Lp3 Dup	2.50	na	na	na

Appendix 4. Recovery Percentages (±Standard Deviation) of Mercury and Selenium in Standard Reference Materials, 2020

Table 4.1. Recovery percentages (±standard deviation) of mercury and selenium in standard reference materials, 2020.

[Sources of reference materials: NIST 2976, National Institute of Science and Technology (NIST; https://www.nist.gov); TORT-3, PACS-3, MESS, National Research Council Canada (NRCC; https://nrc.canada.ca); mean ±uncertainty. See NRCC and NIST for definition of uncertainty value. Abbreviations: mg/kg, milligram per kilogram; SD, standard deviation; %, percent]

Reference material	Sample type	Element	Sample size	Certified value (mg/kg)	Recovery mean ±SD (%)
TORT-3	Biological tissue	Mercury	2	0.29	85±0
NIST 2976	Biological tissue	Mercury	2	0.06	90±2
		Selenium	3	1.8	93±2
PACS-3	Sediment	Mercury	2	2.98	102±7
TORT-3	Biological tissue	Selenium	3	10.9	88±4
MESS	Sediment	Selenium	3	0.72	100±4

Appendix 5. Method Detection Limits and Reporting Levels for Inductively Coupled Plasma Optical Emission Spectrophotometry Methods, in 2020

Table 5.1. Method detection limits and reporting levels for inductively coupled plasma optical emission spectrophotometry methods, 2020.

[Concentrations are reported as milligrams per liter (mg/L). Abbreviations: MDL, method detection limit; MRL, method reporting level]

Sample type	Method limit	Silver	Aluminum	Chromium	Copper	Iron	Nickel	Zinc
Sediment	MDL	0.0005	0.0219	0.0026	0.0037	0.0037	0.0005	0.0006
	MRL	0.0010	0.0439	0.0052	0.0073	0.0075	0.0010	0.0012
Tissue	MDL	0.0005	0.0219	0.0026	0.0022	0.0037	0.0005	0.0006
	MRL	0.0010	0.0439	0.0052	0.0045	0.0075	0.0010	0.0012

Appendix 6. Statistical Summary of Silver and Copper Concentrations in Sediment and Clam *Limecola petalum* Collected at Palo Alto Site, California, in 2020 and in 1977–2020

Table 6.1. Statistical summary of silver and copper concentrations in sediment and clam *Limecola petalum* collected at Palo Alto site, California, in 2020 and in 1977–2020. Data from Cain and others (2022).

[Units for soft tissue of clam (*Limecola petalum*) and for sediment are milligrams per kilogram dry weight. Data in 2020 column are annual (grand) means for calendar year; other columns are statistics for annual (grand) means for 1977–2020. Samples for each year were collected from January to December of that year]

Sample type	Element	Method	2020	Mean	Median	Minimum	Maximum
Sediment	Silver	Partial extraction	0.23	0.49	0.34	0.2	1.62
	Copper	Partial extraction	16.7	22.1	18.3	12.4	55.3
	Copper	Near total	34.0	44.9	43.6	28.0	85.9
Clam tissue	Silver	Tissue digest	2	21	4	2	113
	Copper	Tissue digest	29	77	44	24	283

Appendix 7. Reproduction Data for Clam *Limecola petalum* Collected at Palo Alto Site, California, in 2015–2020

Table 7.1. Reproduction data for clam *Limecola petalum* collected at Palo Alto site, California, in 2015–2020. Data from Cain and others (2022).

[Data are percentages of clams in each stage of reproduction. Spent means clams have released all their gametes. Reproductive is sum of percentage of active, ripe, and spawning stages. Nonreproductive is sum of percentage of inactive and spent stages. Abbreviations: N, number of clams that were analyzed; nd, no data]

Date	Inactive	Active	Ripe	Spawning	Spent	N	Reproductive	Non-reproductive
28-Jan-15	0	0	90	10	0	10	100	0
26-Feb-15	0	0	40	60	0	10	100	0
23-Mar-15	0	0	40	60	0	10	100	0
8-Apr-15	0	0	10	10	80	10	20	80
6-May-15	0	0	0	50	50	10	50	50
8-Jun-15	0	0	0	0	100	10	0	100
1-Jul-15	nd	nd	nd	nd	nd	nd	nd	nd
1-Aug-15	nd	nd	nd	nd	nd	nd	nd	nd
29-Sep-15	90	10	0	0	0	10	10	90
28-Oct-15	10	70	20	0	0	10	90	10
1-Nov-15	nd	nd	nd	nd	nd	nd	nd	nd
21-Dec-15	0	0	100	0	0	10	100	0
19-Jan-16	0	0	100	0	0	10	100	0
16-Feb-16	0	0	60	40	0	10	100	0
30-Mar-16	10	0	20	40	30	10	60	40
27-Apr-16	0	0	40	50	10	10	90	10
31-May-16	0	0	0	20	80	10	20	80
21-Jun-16	0	0	0	10	90	10	10	90
1-Jul-16	nd	nd	nd	nd	nd	nd	nd	nd
1-Aug-16	nd	nd	nd	nd	nd	nd	nd	nd
19-Sep-16	0	60	40	0	0	10	100	0
17-Oct-16	0	70	30	0	0	10	100	0
1-Nov-16	nd	nd	nd	nd	nd	nd	nd	nd
19-Dec-16	0	10	90	0	0	10	100	0
20-Jan-17	0	0	70	30	0	10	100	0
16-Feb-17	0	0	100	0	0	10	100	0
14-Mar-17	0	0	100	0	0	10	100	0
12-Apr-17	0	0	20	80	0	10	100	0
10-May-17	0	0	0	40	60	10	40	60
12-Jun-17	30	30	0	0	40	10	30	70
1-Jul-17	nd	nd	nd	nd	nd	nd	nd	nd

Table 7.1. Reproduction data for clam *Limecola petalum* collected at Palo Alto site, California, in 2015–2020. Data from Cain and others (2022).—Continued

Date	Inactive	Active	Ripe	Spawning	Spent	N	Reproductive	Non-reproductive
1-Aug-17	nd	nd	nd	nd	nd	nd	nd	nd
6-Sep-17	40	60	0	0	0	10	60	40
18-Oct-17	0	30	60	10	0	10	100	0
1-Nov-17	nd	nd	nd	nd	nd	nd	nd	nd
11-Dec-17	0	33.3	55.6	11.1	0	9	100	0
9-Jan-18	0	0	90	10	0	10	100	0
20-Feb-18	0	20	50	30	0	10	100	0
21-Mar-18	0	0	80	20	0	10	100	0
24-Apr-18	0	0	30	50	20	10	80	20
22-May-18	0	0	10	10	80	10	20	80
19-Jun-18	30	70	0	0	0	10	70	30
1-Jul-18	nd	nd	nd	nd	nd	nd	nd	nd
1-Aug-18	nd	nd	nd	nd	nd	nd	nd	nd
12-Sep-18	40	50	10	0	0	10	60	40
10-Oct-18	0	80	20	0	0	10	100	0
1-Nov-18	nd	nd	nd	nd	nd	nd	nd	nd
17-Dec-18	0	0	100	0	0	10	100	0
19-Jan-19	0	0	100	0	0	10	100	0
25-Feb-19	0	0	0	80	20	10	80	20
25-Mar-19	0	0	90	10	0	10	100	0
24-Apr-19	0	0	0	80	20	10	80	20
20-May-19	0	0	0	40	60	10	40	60
19-Jun-19	0	0	0	0	100	10	0	100
1-Jul-19	nd	nd	nd	nd	nd	nd	nd	nd
1-Aug-19	nd	nd	nd	nd	nd	nd	nd	nd
17-Sep-19	44.4	55.6	0	0	0	9	55.6	44.4
28-Oct-19	0	90	10	0	0	10	100	0
1-Nov-19	nd	nd	nd	nd	nd	nd	nd	nd
20-Dec-19	30	40	30	0	0	10	70	30
18-Jan-20	10.0	80.0	10.0	0.0	0.0	10.0	90.0	10.0
17-Feb-20	0.0	0.0	100.0	0.0	0.0	10.0	100.0	0.0
10-Mar-20	0.0	0.0	70.0	20.0	10.0	10.0	90.0	10.0
1-Apr-20	nd	nd	nd	nd	nd	nd	nd	nd
13-May-20	0.0	0.0	0.0	50.0	50.0	10.0	50.0	50.0
23-Jun-20	0.0	0.0	0.0	40.0	60.0	10.0	40.0	60.0
1-Jul-20	nd	nd	nd	nd	nd	nd	nd	nd
1-Aug-20	nd	nd	nd	nd	nd	nd	nd	nd
19-Sep-20	60.0	40.0	0.0	0.0	0.0	10.0	40.0	60.0
22-Oct-20	0.0	90.0	10.0	0.0	0.0	10.0	100.0	0.0
1-Nov-20	nd	nd	nd	nd	nd	nd	nd	nd
11-Dec-20	0.0	0.0	100.0	0.0	0.0	10.0	100.0	0.0

Appendix 8. Complete List of Benthic Species Found at Palo Alto Site, California, in 2020

Table 8.1. Complete list of benthic species found at Palo Alto site, California, in 2020. Data from Cain and others (2022).

[Three samples are taken at each sampling event. Mean abundance ($\bar{x}$) and standard deviation (SD) of three samples are shown]

Taxon	1/17/2020		2/13/2020		5/12/2020		6/10/2020		7/8/2020		8/5/2020		9/2/2020		10/1/2020		12/9/2020	
	$\bar{x}$	SD	$\bar{x}$	SD	$\bar{x}$	SD	$\bar{x}$	SD	$\bar{x}$	SD	$\bar{x}$	SD	$\bar{x}$	SD	$\bar{x}$	SD	$\bar{x}$	SD
PHYLUM MOLLUSCA																		
Class Bivalvia																		
Order Myida																		
Family Corbulidae																		
Potamocorbula amurensis	0.7	0.6	0.3	0.6	63.7	20.1	99.0	23.6	87.7	25.3	55.3	13.3	47.0	14.7	8.7	2.1	3.7	2.1
Order Veneroida																		
Family Tellinidae																		
Limecola petalum	1.0	0.0	0.7	1.2	2.7	2.1	2.7	3.1	1.7	1.2	1.0	1.0	1.7	1.5	1.0	1.0	2.3	1.2
Family Veneridae																		
Gemma gemma	126.0	37.2	39.7	68.7	293.0	32.4	253.3	118.4	176.0	28.6	28.6	284.3	213.0	66.5	248.0	191.7	816.0	73.0
Class Gastropoda																		
Gastropoda spp.	0.0	0.0	0.0	0.0	0.3	0.6	2.0	0.0	1.3	0.6	4.0	3.5	2.0	2.0	5.3	5.0	4.7	3.5
PHYLUM ANNELIDIA																		
Class Clitellata																		
Oligochaeta spp.	51.3	36.2	3.3	4.2	18.7	6.7	7.3	4.6	17.7	14.6	15.3	18.0	19.3	9.9	8.3	8.7	37.0	32.8
Class Polychaeta																		
Order Phyllodocida																		
Family Nereididae																		
Alitta succinea	0.7	0.6	0.3	0.6	0.0	0.0	0.3	0.6	0.3	0.6	1.0	1.0	0.3	0.6	1.0	0.0	0.0	0.0
Family Phyllidocidae																		
Eteone lighti	3.3	0.6	0.0	0.0	8.7	2.1	17.7	5.0	9.7	2.1	6.0	3.6	4.0	1.0	2.3	2.3	4.0	1.7

Table 8.1. Complete list of benthic species found at Palo Alto site, California, in 2020. Data from Cain and others (2022).

Taxon	1/17/2020		2/13/2020		5/12/2020		6/10/2020		7/8/2020		8/5/2020		9/2/2020		10/1/2020		12/9/2020	
	$\bar{x}$	SD	$\bar{x}$	SD	$\bar{x}$	SD	$\bar{x}$	SD	$\bar{x}$	SD	$\bar{x}$	SD	$\bar{x}$	SD	$\bar{x}$	SD	$\bar{x}$	SD
PHYLUM ANNELIDIA—Continued																		
Infraclass Scolecida																		
Family Capitellidae																		
Heteromastus filiformis	6.3	2.5	0.0	0.0	6.0	1.0	2.7	4.6	0.7	0.6	0.3	0.6	4.0	3.0	0.0	0.0	4.0	3.5
Family Cossuridae																		
Order Spionida																		
Family Spionidae																		
Streblospio benedicti	1.0	0.0	0.0	0.0	9.7	6.1	0.0	0.0	0.0	0.0	0.7	1.2	0.7	1.2	0.0	0.0	3.0	3.6
Order Terebellida																		
Family Cirratulidae																		
Cirratulidae spp.	0.0	0.0	0.0	0.0	1.7	1.5	0.3	0.6	0.7	0.6	1.3	2.3	0.7	1.2	0.0	0.0	0.7	0.6
PHYLUM ARTHROPODA																		
Class Malacostraca																		
Order Amphipoda																		
Family Ampeliscidae																		
Ampelisca abdita	0.0	0.0	0.0	0.0	0.3	0.6	1.0	1.0	0.3	0.6	0.0	0.0	0.0	0.0	0.7	0.6	0.7	0.6
Family Aoridae																		
Grandidierella japonica	1.7	2.1	0.7	1.2	1.0	1.7	4.7	1.2	0.7	1.2	3.7	2.1	6.0	4.0	23.7	6.0	18.7	2.5
Family Corophiidae																		
Monocorophium acherusicum	0.0	0.0	0.0	0.0	0.0	0.0	0.0	0.0	0.0	0.0	0.0	0.0	0.0	0.0	4.7	2.3	12.3	11.4
Order Cumacea																		
Family Leuconidae																		
Nippoleucon hinumensis	76.3	11.0	18.3	29.2	68.7	24.3	135.7	39.1	35.3	10.6	15.7	2.5	4.3	2.3	8.7	3.5	54.7	4.6
Order Isopoda																		
Family Idoteidae																		
Synidotea laevidorsalis	0.0	0.0	0.0	0.0	0.0	0.0	0.0	0.0	0.3	0.6	0.7	1.2	0.0	0.0	0.3	0.6	0.0	0.0

Table 8.1. Complete list of benthic species found at Palo Alto site, California, in 2020. Data from Cain and others (2022).

Taxon	1/17/2020		2/13/2020		5/12/2020		6/10/2020		7/8/2020		8/5/2020		9/2/2020		10/1/2020		12/9/2020	
	$\bar{x}$	SD	$\bar{x}$	SD	$\bar{x}$	SD	$\bar{x}$	SD	$\bar{x}$	SD	$\bar{x}$	SD	$\bar{x}$	SD	$\bar{x}$	SD	$\bar{x}$	SD
PHYLUM ARTHROPODA—Continued																		
Family Sphaeromatidae																		
Gnorimosphaeroma oregonensis	0.0	0.0	0.3	0.6	0.0	0.0	0.7	1.2	0.3	0.6	0.0	0.0	0.0	0.0	0.0	0.0	0.0	0.0
Order Tanaidacea																		
Class Maxillopoda																		
Order Sessilia																		
Balanus spp.	0.0	0.0	0.0	0.0	0.0	0.0	1.0	1.0	0.0	0.0	0.0	0.0	0.0	0.0	0.0	0.0	0.0	0.0
Class Ostracoda																		
Order Myodocopida																		
Family Sarsiellidae																		
Eusarsiella zostericola	0.3	0.6	0.3	0.6	1.3	0.6	0.0	0.0	0.0	0.0	3.3	3.5	5.0	2.0	11.7	5.1	21.7	9.1

Appendix 9. Benthic Species Name Changes as of 2020

Table 9.1. Benthic species name changes as of 2020.

[Current species names from WoRMS Editorial Board (2020)]

Current species name	Formerly documented as
PHYLUM CNIDARIA	
Class Anthozoa	
Order Actiniaria	
Actiniaria spp.	*Anthozoa*, unid. *Actiniaria*, *Actiniaria* unid. spp.
PHYLUM PLATYHELMINTHES	
Platyhelminthes spp.	*Turbellaria*, *Turbellaria* unid. spp.
PHYLUM NEMATODA	
Nematoda spp.	*Nematoda* unid. spp.
PHYLUM ANNELIDA	
Class Clitellata	
Naididae spp.	*Naididae*, *Naididae* unid. spp.
Oligochaeta spp.	*Oligochaeta*, unid. *Oligochaeta* family, *Oligochaeta* unid. spp.
Class Polychaeta	
Polychaeta spp.	unid. *Polychaeta*, *Polychaeta*, *Polychaeta* unid. spp.
Order Eunicida	
Family Dorvilleidae	
Schistomeringos longicornis	*Dorvillea longicornis*
Schistomeringos annulata	*Dorvillea annulata*, *Dorvillea longicornuta*, *Schistomeringos longicornuta*, *Dorvillea rudolphi*
Order Phyllodocida	
Family Glyceridae	
Glycera spp.	*Glycera* unid. spp.
Family Goniadidae	
Glycinde picta	*Glycinde polygnatha*
Glycinde sp. SF1	*Glycinde* unid. sp. SF1
Glycinde spp.	*Glycinde* unid. spp.
Family Nereididae	
Alitta succinea	*Neanthes succinea*
Family Phyllidocidae	
Eteone spp.	*Eteone ?Californica*, *Eteone* unid. spp.
Family Syllidae	
Sphaerosyllis unid. sp. A	*Sphaerosylis* spp.
Infraclass Scolecida	
Family Capitellidae	
Capitella capitata complex	*Capitella "capitata"*
Family Maldanidae	
Maldanidae spp.	unid. *Maldanidae*, *Maldanidae* unid. spp.
Order Sabellida	
Family Sabellidae	
Euchone spp.	*Euchone* unid. spp.

Table 9.1. Benthic species name changes as of 2020.—Continued

Current species name	Formerly documented as
PHYLUM ANNELIDA—Continued	
Order Spionida	
Family Spionidae	
Polydora cornuta	*Polydora lighti*, *Polydora ligni*
Polydora spp.	*Polydora* unid. spp.
Spionidae spp.	unid. *Spionidae*, *Spionidae spp.*, *Spionidae* unid. spp.
Order Terebellida	
Family Cirratulidae	
Cirratulidae spp.	*Tharyx* spp. ?, *Cirratulidae*, *Cirratulidae* unid. spp.
PHYLUM ARTHROPODA	
Class Insecta	
Chironomidae spp.	*Chironomidae*, *Chironomidae* unid. spp.
Class Maxillopoda	
Calanoida spp.	*Calanoida*, *Calanoida* unid. spp.
Harpacticoida spp.	*Harpacticoida*, *Harpacticoida* unid. spp.
Class Malacostraca	
Order Amphipoda	
Family Ampithoidae	
Ampithoe spp.	*Ampithoe* unid. spp.
Family Anisogammaridae	
Eogammarus confervicolus	*Anisogammarus confervicolus*
Family Corophiidae	
Americorophium spinicorne	*Corophium spinicorne*
Corophiidae spp.	*Corophium* spp., *Corophiidae* unid. spp.
Corophium spp.	*Corophiidae unid.*, *Corophium* unid. spp.
Monocorophium acherusicum	*Corophium ascherusicum*
Monocorophium insidiosum	*Corophium insidiosum*
Monocorophium spp.	*Corophium ?insidiosum*, *Corophium* spp. (female and juvenile), *Corophium* spp. (male), *Monocorophium* unid. spp.
Family Melitidae	
Melita spp.	*Melita* unid. spp.
Family Oedicerotidae	
Americhelidium spp.	*Synchelidium* spp., *Americhelidium* unid. spp.
Order Cumacea	
Family Leuconidae	
Nippoleucon hinumensis	*Hemileucon hinumensis*
Order Decapoda	
Family Callianassidae	
Callianassidae spp.	*Callianassidae*, *Callianassidae* unid., *Callianassidae* unid. spp.
Order Isopoda	
Family Idoteidae	
Synidotea spp.	*Synidotea* unid. spp.
Family Sphaeromatidae	
Sphaeromatidae spp.	*Sphaeromatidae (juv.)*, *Sphaeromatidae* unid., *Dynamella* spp., *Sphaeromatidae* unid. spp.

Table 9.1. Benthic species name changes as of 2020.—Continued

Current species name	Formerly documented as
PHYLUM ARTHROPODA—Continued	
Order Mysida	
Mysida spp.	*Mysidacea*, *Mysidacea* spp., *Mysidacea* unid. spp.
Order Tanaidacea	
Family Tanaididae	
Sinelobus spp.	*Sinelobus stanfordi*, *Tanais* spp., *Sinelobus* unid. spp.
Class Maxillopoda	
Order Sessilia	
Balanomorpha spp.	*Balanus ?aquila*, *Balanus* spp., unid. *Balanomorpha*, *Balanomorpha* unid., *Balanomorpha* unid. spp.
Cirripedia spp.	*Cirripedia*, *Cirripedia* unid. spp.
Class Ostracoda	
Order Myodocopida	
Family Sarsiellidae	
Eusarsiella zostericola	*Sarsiella zostericola*
Order Podocopida	
Family Cytherideidae	
Cyprideis unid. spp.	*Cyprideis* spp.
PHYLUM MOLLUSCA	
Class Bivalvia	
Bivalvia spp.	*Bivalvia* unid. spp., unid. *Bivalvia*
Order Myida	
Family Corbulidae	
Potamocorbula amurensis	*Corbula amurensis*
Order Veneroida	
Family Tellinidae	
Limecola petalum	*Limecola balthica, Limecola petalum*
Limecola spp.	*Limecola* unid. spp., *Limecola* spp.
Tellinidae spp.	*Tellinidae* unid. spp., *Tellinidae*
Class Gastropoda	
Gastropod unid. sp. *B*	*unid. Gastropoda* B
Order Cephalaspidea	
Family Philinidae	
Philine spp.	*Philine* unid. spp.
Order Heterostropha	
Family Pyramidellidae	
Boonea bisuturalis	*Odetta bisuturalis*, *Odostomia fetella*
Pyramidellidae spp.	*Odostomia* spp., *Pyramidellidae*, unid. *Gastropod* A, *Pyramidellidae* unid. spp.
Family Nassariidae	
Tritia obsoleta	*Nassarius obsolete, Ilyanassa obsoletas*

Moffett Field Publishing Service Center, California
Manuscript approved Feburary 21, 2023
Edited by Alex S. Lyles
Layout and design by Kimber Petersen
Illustration support by Cory Hurd

ISSN 2331-1258 (online)
https://doi.org/10.3133/ofr20231017